Electrostatic Calibrations and Casimir Force Measurements: the Case of Ge Samples in a Torsion Balance Set-up

Diego A. R. Dalvit
Theoretical Division
Los Alamos National Laboratory

Collaborators

LANL - Yale collaboration:

Steve Lamoreaux

Alex Sushkov

Woo-Joong Kim (now @ Seattle University)

LANL - Dartmouth collaboration:

Roberto Onofrio

Funding provided by:

Outline of this Talk

- New torsional balance apparatus at Yale
- Electrostatic calibrations for Casimir measurements
  - Contact potential differences - Varying minimizing potential
  - Surface potential patches and electrostatic force *residuals*
- Casimir force between Ge plates
  - Theory - several theoretical models
  - Experiment - evidence of electric residual forces and Casimir
- Casimir force between Au plates
  - *Preliminary* results - Plasma or Drude?

New Casimir Apparatus at Yale

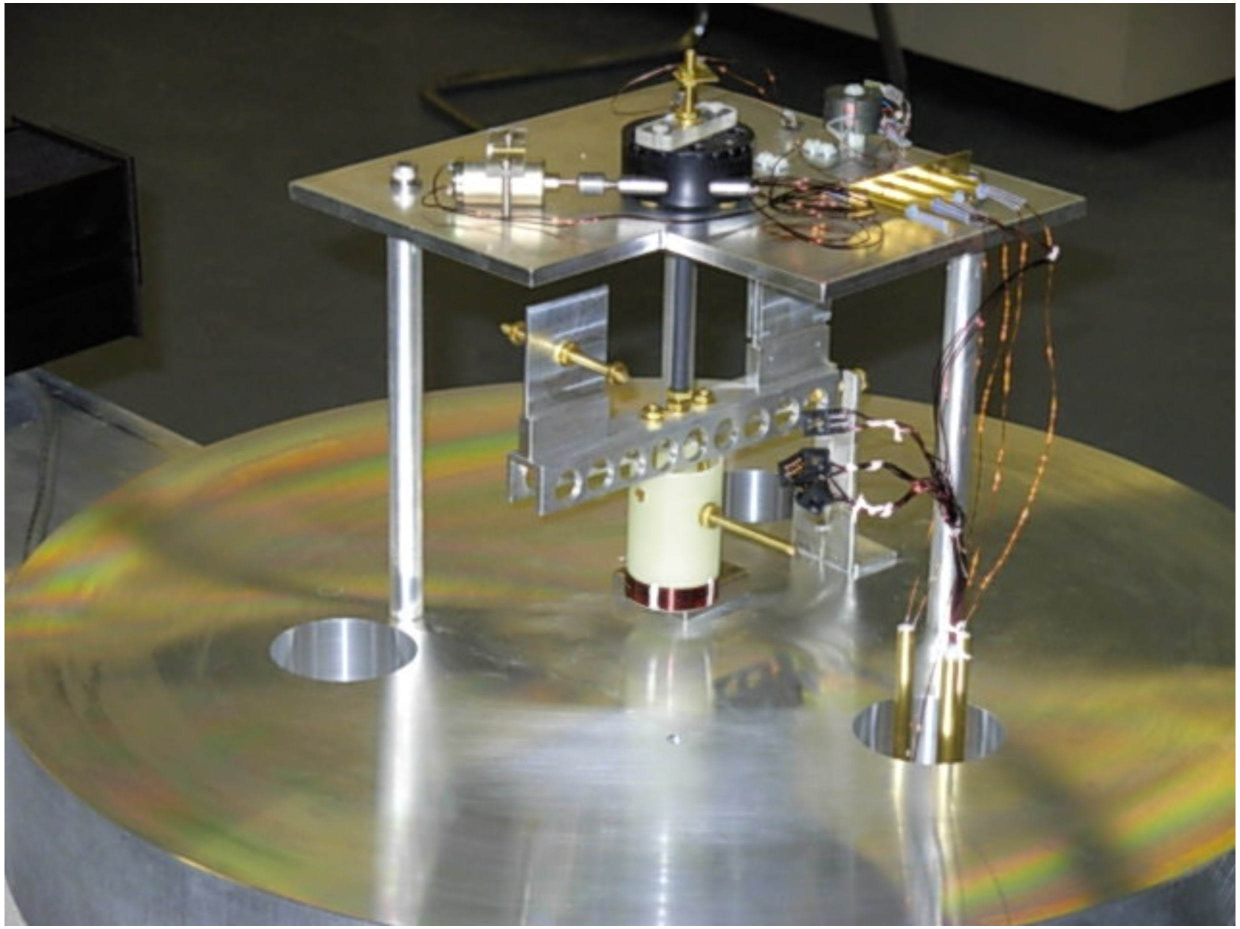

Torsional Pendulum Set-up

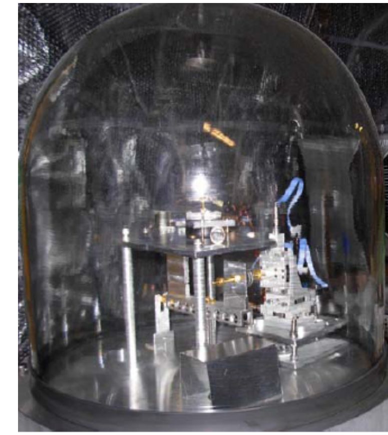

✱ Upgrade of Lamoreaux's 1997 experiment

- shorter wire length ($l = 2.5 \text{ cm}$) for reduced tilt
- improved vacuum ($P = 5 \times 10^{-7} \text{ torr}$)
- improved vibration oscillation
- Motion XYZ stage with 8 nm resolution
- NdFeB magnet at bottom to damp swinging modes of the pendulum at natural frequency of 3 Hz

✱ Sphere-plane geometry $R = 15.1 \text{ cm}$

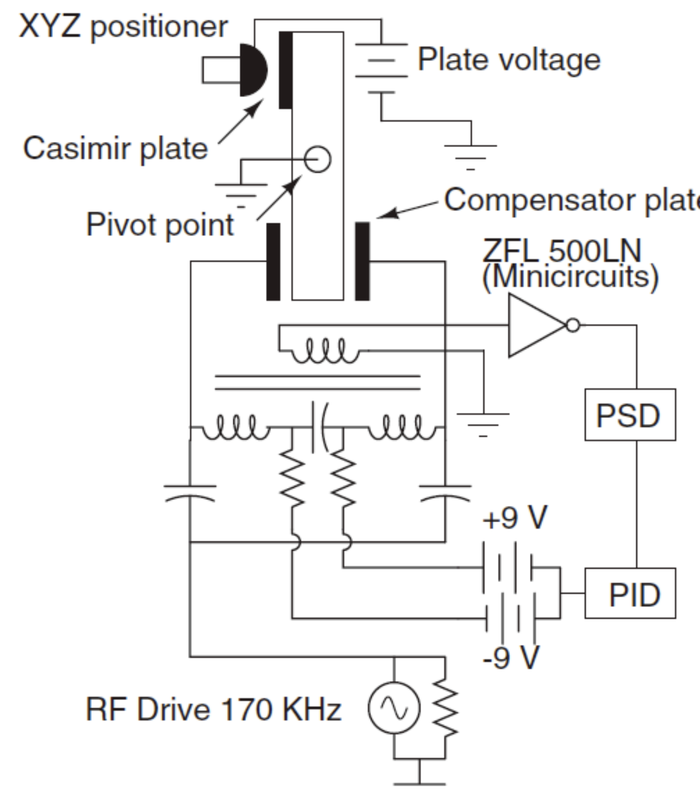

An imbalance in capacitance is amplified and sent to a phase sensitive detector (PSD), which generates error signals.

A proportional integro-differential (PID) controller provides a feedback correction voltage $S_{\text{PID}}(d, V_a)$ to the compensator plates, restoring equilibrium.

$$F \propto (S_{\text{PID}} + 9V)^2 \approx (9V)^2 + 2S_{\text{PID}} \times 9V$$

The correction voltage is the physical observable, and it is proportional to the force between the Casimir plates

Electrostatic Calibrations

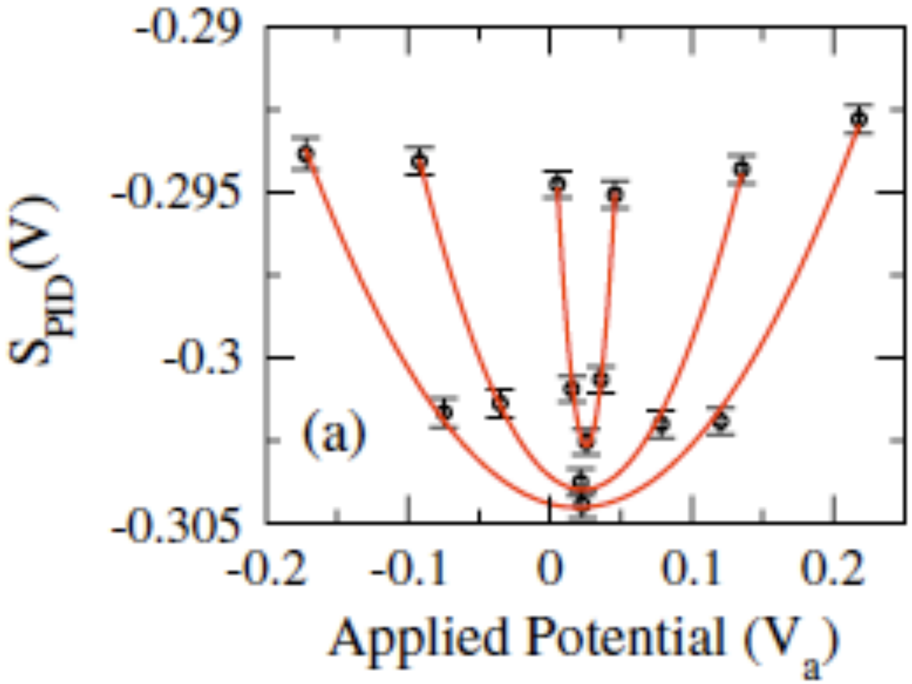

Kim, Sushkov, DD, Lamoreaux, PRL **103**, 060401 (2009)

Typical Casimir Measurement

$$S_{\mathrm{PID}}(d, V_a) = S_{\mathrm{dc}}(d \to \infty) + S_a(d, V_a) + S_r(d)$$

force-free component of signal at large separations

electrostatic signal in response to an applied external voltage

residual signal due to distance-dependent forces, e.g. Casimir

The electrostatic signal between the spherical lens and the plate, in PFA $(d \ll R)$ is

$$S_a(d, V_a) = \pi \epsilon_0 R (V_a - V_m)^2 / \beta d$$

β force-voltage conversion factor

This signal is minimized ($S_a = 0$) when $V_a = V_m$, and the electrostatic minimizing potential V_m is then defined to be the contact potential between the plates.

Typical Casimir Measurement

Los Alamos
NATIONAL LABORATORY

$$S_{\text{PID}}(d, V_a) = S_{\text{dc}}(d \to \infty) + S_a(d, V_a) + S_r(d)$$

force-free component of signal at large separations

electrostatic signal in response to an applied external voltage

residual signal due to distance-dependent forces, e.g. Casimir

The electrostatic signal between the spherical lens and the plate, in PFA $(d \ll R)$ is

$$S_a(d, V_a) = \pi\epsilon_0 R(V_a - V_m)^2/\beta d$$

β force-voltage conversion factor

This signal is minimized ($S_a = 0$) when $V_a = V_m$, and the electrostatic minimizing potential V_m is then defined to be the contact potential between the plates.

Naive picture

Counterbias $V_a = V_m$ fixed at large separations, and *assumed to be distance-independent* → electrostatic force is supposedly *nullified*

"Parabola" measurements

Calibration routine (Iannuzzi et al, PNAS 04)

A range of plate voltages V_a is applied, and at a given nominal absolute distance the response is fitted to a parabola

$$S_{\mathrm{PID}}(d, V_a) = S_0 + k(V_a - V_m)^2$$

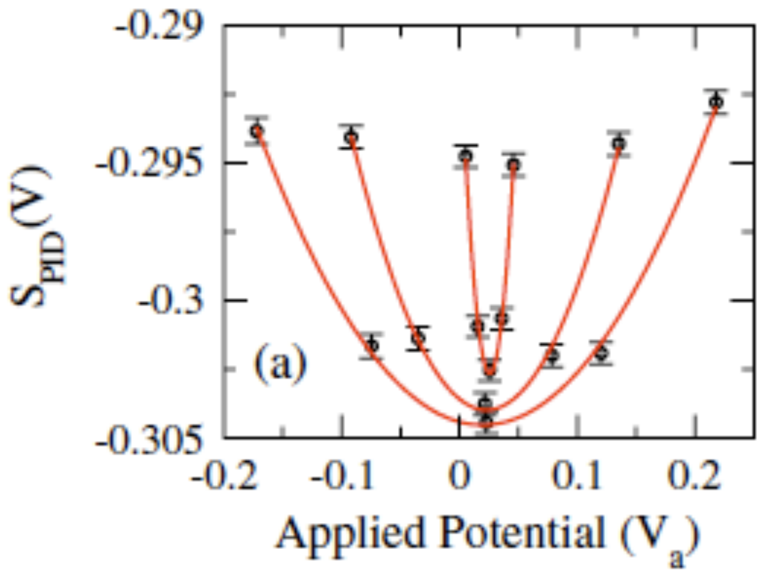

Fitting parameters

$k = k(d)$ ⟶ voltage-force calibration factor + absolute distance

$V_m = V_m(d)$ ⟶ distance-dependent minimizing potential

$S_0 = S_0(d)$ ⟶ force residuals: electrostatic + Casimir + non-Newtonian gravity + ...

This procedure is repeated at decremental distances, from150 um down to 500 nm, completing a single experimental run.

Note: The maximum force gradient for feedback system stability is 5 nm/um, limiting the minimum distance to 500 nm.

Curvature Parameter $k(d)$

From the curvature of the different parabolas one obtains k(d)

$$\boxed{k(d) = \frac{\pi\epsilon_0 R/\beta}{d}}$$

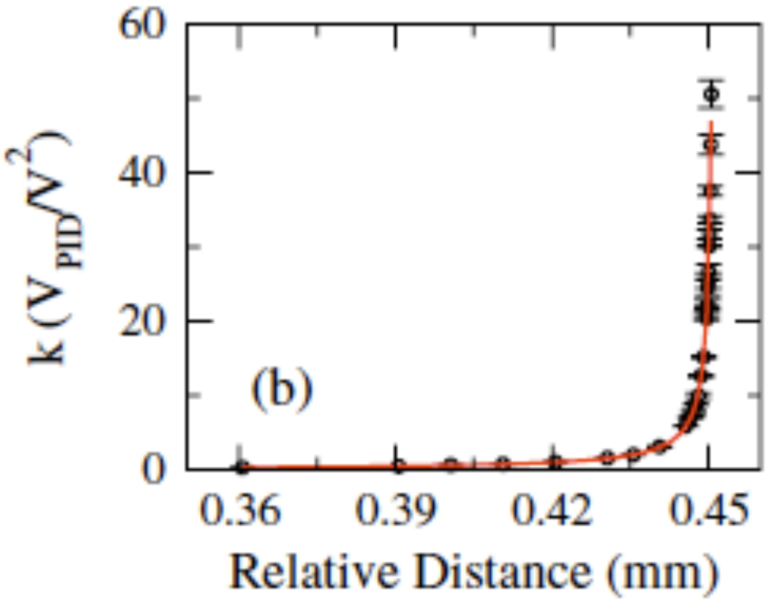

☑ Force-voltage calibration factor

$$\beta = (1.35 \pm 0.04) \times 10^{-7}\ \mathrm{N/V}$$

☑ Sphere-plane absolute distance

$$d = d_0 - d_{\mathrm{rel}}$$

Typical uncertainty in position is about 10% at a given distance

Some further details:

- Average $\chi^2 = 1.2$
- Drift of about 5 um in 3 weeks
- Single sweep suffers about 20nm drift (less than 5% at the closest approach of 500nm)

Varying Minimizing Potential

Our Ge data shows a *distance-dependent* minimizing potential, of the order of 6 mV over 100 um.

$$\boxed{V_m = V_m(d)}$$

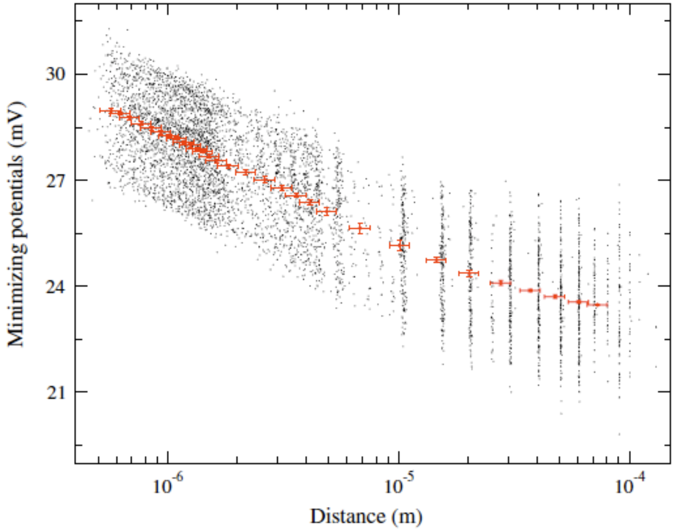

Therefore, a fixed counterbias would be incorrect!

Varying Minimizing Potential

Our Ge data shows a *distance-dependent* minimizing potential, of the order of 6 mV over 100 um.

$$\boxed{V_m = V_m(d)}$$

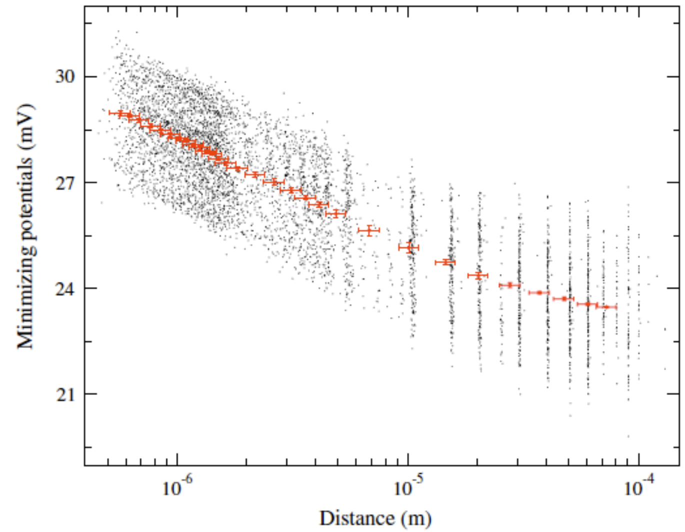

Therefore, a fixed counterbias would be incorrect!

Similar behavior has been observed in a number of experiments with Au plates (both with macro and micro spheres), including

Onofrio's group

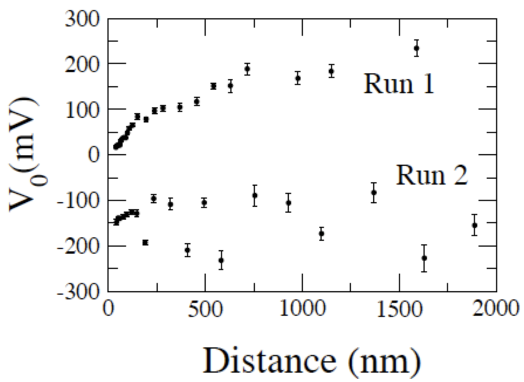

Capasso's group

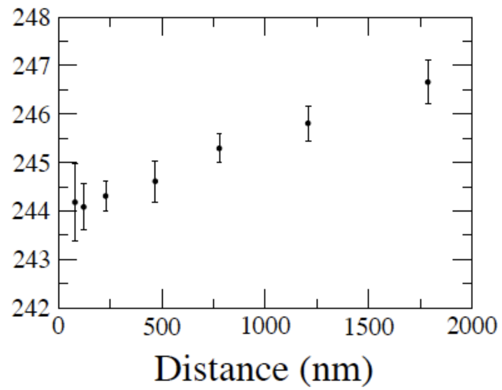

Chevrier's group

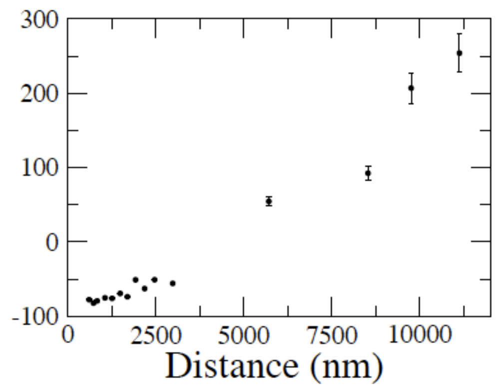

Iannuzzi's group

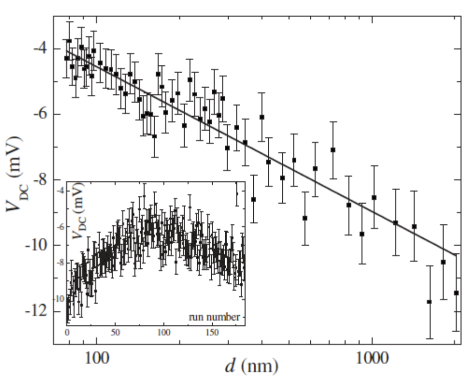

(See Kim, Brown-Hayes, DD, Brownell, Onofrio, PRA 08, 09)

Force Residuals

Residuals from Coulomb force obtained from the value of the PID signal at the minima of each parabola,

$$S_0(d) \rightarrow F_r(d)$$

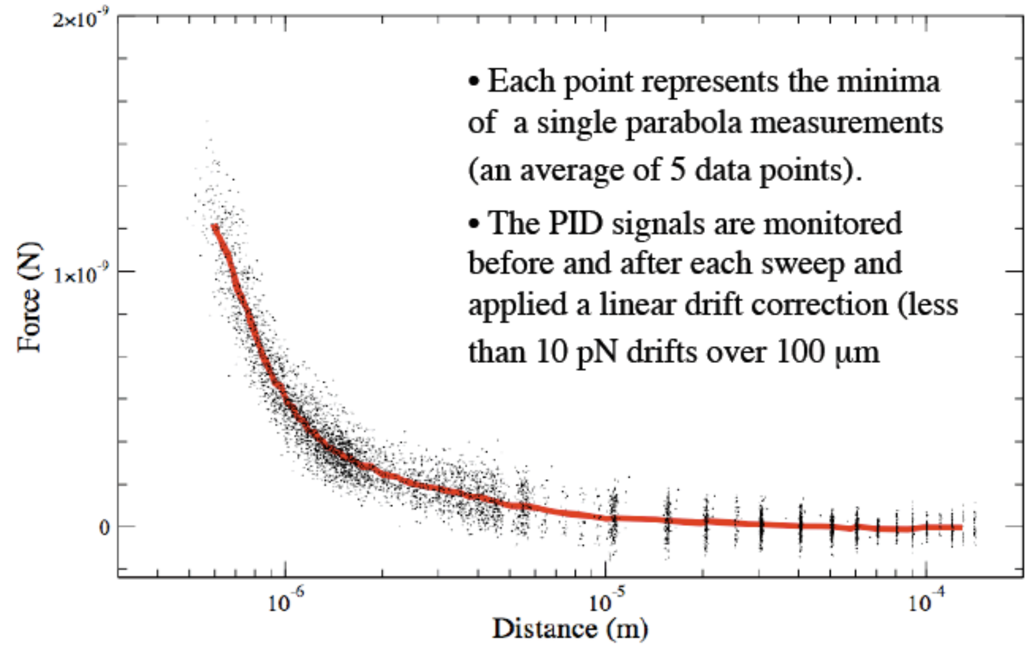

In our experiment, these force residuals are <u>*too large*</u> to be explained just by the Casimir-Lifshitz force between the Ge plates.

In fact, the experimental data shows a $1/d$ force residual at distances $d > 5\mu\mathrm{m}$, where the Casimir force should be negligible.

Force Residuals

Residuals from Coulomb force obtained from the value of the PID signal at the minima of each parabola,

$$S_0(d) \rightarrow F_r(d)$$

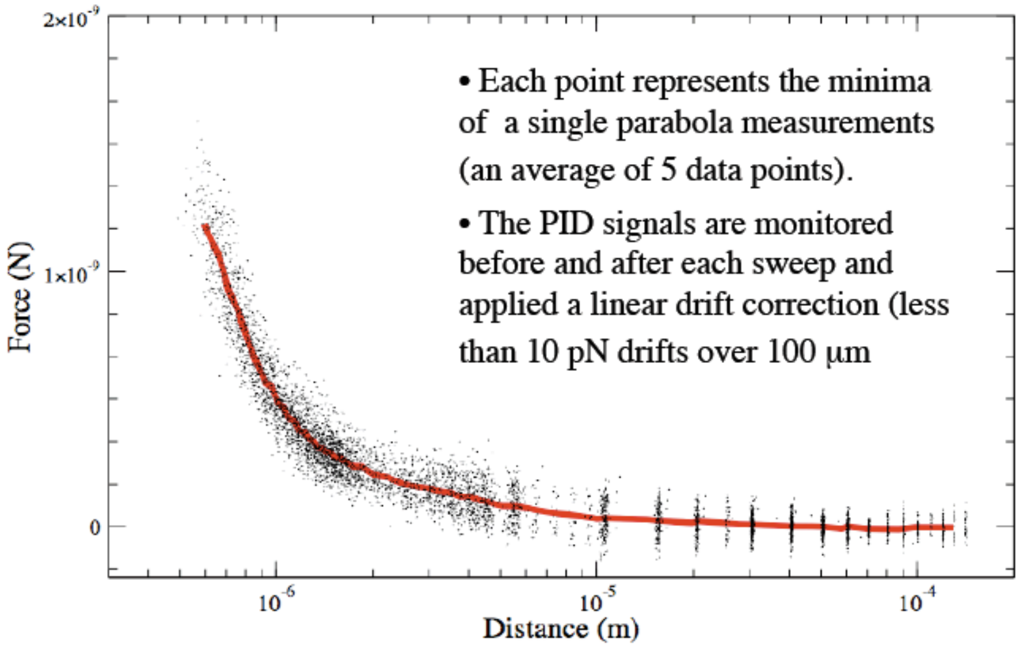

In our experiment, these force residuals are *too large* to be explained just by the Casimir-Lifshitz force between the Ge plates.

In fact, the experimental data shows a $1/d$ force residual at distances $d > 5\mu\text{m}$, where the Casimir force should be negligible.

What is the origin of the varying minimizing potential?

What is the origin of the additional force residual?

Electrostatic Patches & Residuals

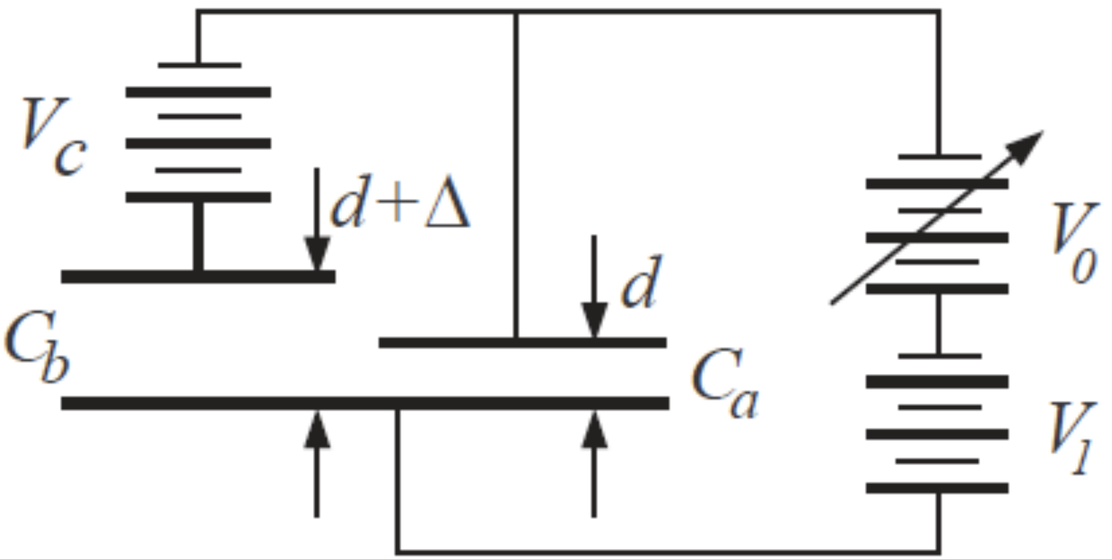

Kim, Sushkov, DD, Lamoreaux, arXiv:0905.3421

Surface Potentials & $V_m(d)$

The surface of a conductor is an equipotential only for a perfectly clean surface of a homogeneous system cut along one of its crystalline planes.

It is NOT the case for any real material.

- oxide layers in "dirt" films
- local variations in the crystalline structure
- different work functions

Electrostatic force (in PFA, $R \gg d$):

$$F(d, V_0) = \frac{\epsilon_0}{2} \int_0^{2\pi} d\varphi \int_0^R r dr \frac{(V(r,\varphi) + V_0)^2}{(d + r^2/2R)^2}$$

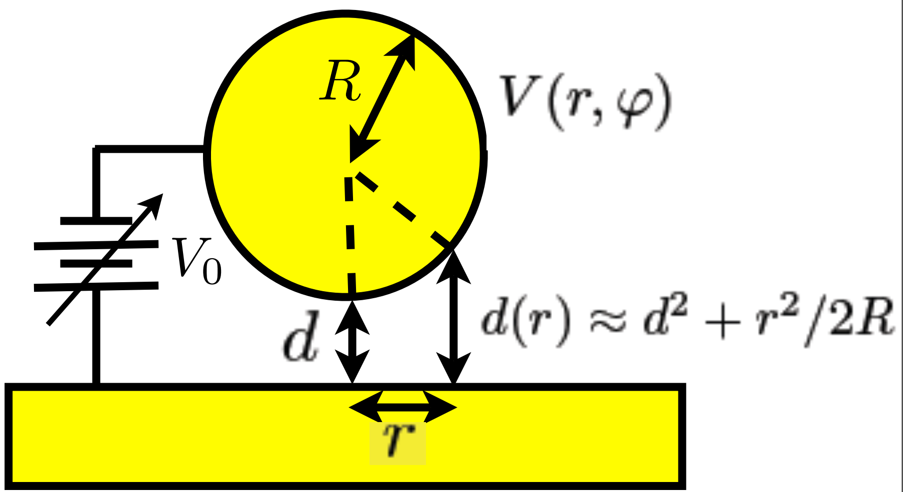

Minimized force at a fixed distance determines the minimizing potential $V_m(d)$

$$0 = \left.\frac{\partial F(d, V_0)}{\partial V_0}\right|_{V_0 = V_m} = \epsilon_0 \int_0^{2\pi} d\varphi \int_0^R r dr \frac{V(r,\varphi) + V_m}{(d + r^2/2R)^2}$$

and

$$\frac{\partial^2 F(d, V_0)}{\partial V_0^2} = 2\pi\epsilon_0 \int_0^R dr \frac{r}{(d + r^2/2R)^2} \approx \frac{2\pi R\epsilon_0}{d}$$

☑ Surface patches DO NOT interfere with distance calibration!

$V_m(d)$ & Residual Elec. Force. I

Los Alamos NATIONAL LABORATORY

A toy model illustrating the mechanism for the generation of $V_m(d)$ and $F^{\rm el}_{\rm res}(d)$

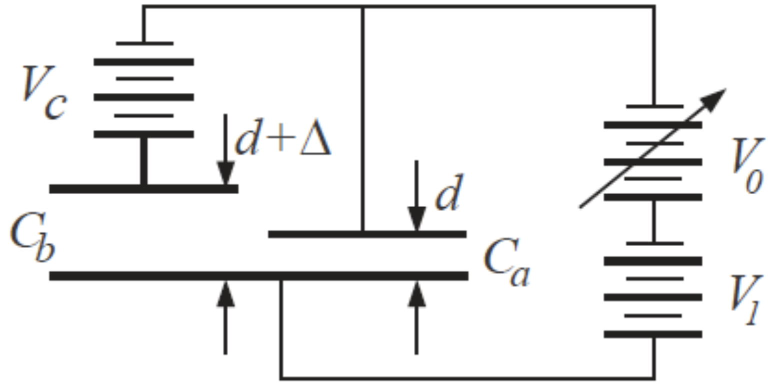

Force on lower plate:

$$F(d, V_0) = -\frac{1}{2}C'_a V_0^2 - \frac{1}{2}C'_b(V_0 + V_c)^2$$

(V_0 is varied, V_c a fixed property of the plates)

$$C'_a = -\epsilon_0 A/d^2$$
$$C'_b = -\epsilon_0 A/(d+\Delta)^2$$

When force is minimized, one gets a varying minimizing potential and a varying electrostatic residual force.

$$\left.\frac{\partial F(d,V_0)}{\partial V_0}\right|_{V_0=V_m} = 0 \;\Rightarrow\; V_m(d) = -\frac{C'_b V_c}{C'_a + C'_b} = \; -V_c\frac{d^2}{d^2+(d+\Delta)^2}$$

$$F^{\rm el}_{\rm res}(d) \;=\; F(d, V_0 = V_m(d)) = \frac{\epsilon_0 A}{2}\,\frac{V_m^2(d)[d^2+(d+\Delta)^2]}{d^4} \propto \frac{1}{d^4} \text{ for } \Delta \gg d$$

In reality, measurements can determine $V_m(d)$ up to an overall constant: $V_m(d) \to V_m(d) + V_1$

$V_m(d)$ & Residual Elec. Force. II

Los Alamos NATIONAL LABORATORY

Sphere-plane case: $C_a'(d) = -2\pi\epsilon_0 R/d$

Dividing the sphere into infinitesimal areas, each with a random potential, and integrating over the surface to get the net residual force (as in PFA), we get

$$\boxed{F_{\rm res}^{\rm el}(d) = \pi\epsilon_0 R\,\frac{[V_m(d)+V_1]^2}{d}}$$

Important message from this analysis:

☑ Minima of parabolas DO NOT nullify all possible electrostatic forces between plates!

Electrostatic Patch Effects. I

The patch effect is a possible systematic limitation to Casimir force measurements (Speake and Trenkel, PRL 03).

We have derived a simpler formulation of the problem (arXiv:0905.3421)

Plane-plane geometry:

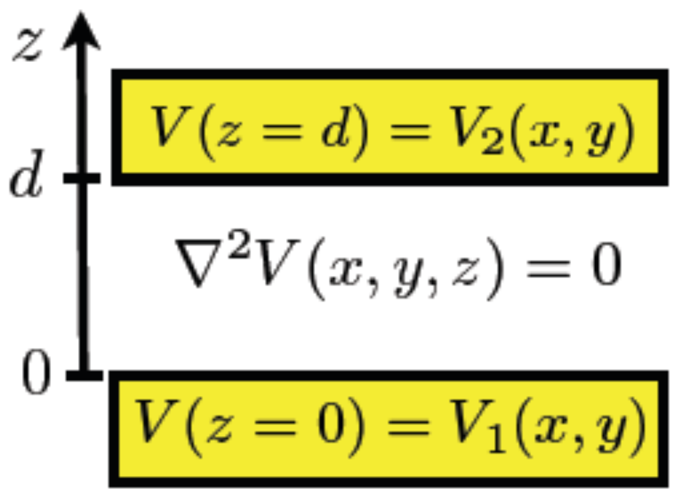

$$V(x,y,z)=X(x)Y(y)Z(z)$$

$$\frac{1}{X}\frac{d^2X}{dx^2}=-\alpha^2;\quad \frac{1}{Y}\frac{d^2Y}{dy^2}=-\beta^2;\quad \frac{1}{Z}\frac{d^2Z}{dz^2}=\gamma^2=\alpha^2+\beta^2$$

$$V_1(x,y)=\int\frac{d^2\mathrm{k}}{(2\pi)^2}V_{1,\mathrm{k}}\cos(k_x x)\cos(k_y y)$$ [idem for $V_2(x,y)$]

$$\boxed{\begin{aligned}V(x,y,z)&=\int\frac{d^2\mathrm{k}}{(2\pi)^2}\frac{\cos(k_x x)\cos(k_y y)}{2\sinh(\gamma d)}\\&\times\left[e^{\gamma z}\left(V_{2,\mathrm{k}}-V_{1,\mathrm{k}}e^{-\gamma d}\right)+e^{-\gamma z}\left(V_{1,\mathrm{k}}e^{\gamma d}-V_{2,\mathrm{k}}\right)\right]\end{aligned}}$$

Electrostatic energy:

$$U_{pp}(d)=\frac{\epsilon_0}{2}\int d^3\mathbf{r}\,|\nabla V|^2$$

Electrostatic Patch Effects. II

Statistical properties for patch potentials:

$$\langle V_{1,\mathbf{k}}\rangle = \langle V_{2,\mathbf{k}}\rangle = \langle V_{2,\mathbf{k}} V_{1,\mathbf{k}'}\rangle = 0;$$
$$\langle V_{1,\mathbf{k}} V_{1,\mathbf{k}'}\rangle = C_{1,\mathbf{k}}\, \delta^2(\mathbf{k}-\mathbf{k}');$$
$$\langle V_{2,\mathbf{k}} V_{2,\mathbf{k}'}\rangle = C_{2,\mathbf{k}}\, \delta^2(\mathbf{k}-\mathbf{k}'),$$

Averaging the interaction energy over different realizations of the stochastic patches, we get

$$\langle U_{pp}\rangle = \frac{\epsilon}{16}\int \frac{d^2\mathbf{k}}{(2\pi)^2}\, \frac{\gamma \sinh(2\gamma d)}{\sinh^2(\gamma d)}\, [C_{1,\mathbf{k}} + C_{2,k}]$$

In the limit of large distances $(kd \gg 1)$, this expression has an asymptotic behavior independent of distance (self-energy of each plate). We remove the potential energy at infinite separation, to get the electrostatic interaction energy due to patch effects

$$\boxed{\langle U_{pp}\rangle = \frac{\epsilon_0}{32\pi}\int_0^\infty dk\, \frac{k^2 e^{-kd}}{\sinh(kd)}\, [C_{1,k} + C_{2,k}]}$$

For large patches $(kd \ll 1)$: $\langle U_{pp}\rangle = \dfrac{\epsilon_0 V_{\mathrm{rms}}^2}{2d}$

For small patches $(kd \gg 1)$: $\langle U_{pp}\rangle \propto e^{-kd}$

Electrostatic Patch Effects. III

Sphere-plane geometry:

To compute the patch effect in the sphere-plane configuration we use PFA for the curvature effect $(d \ll R)$ but leave kd arbitrary

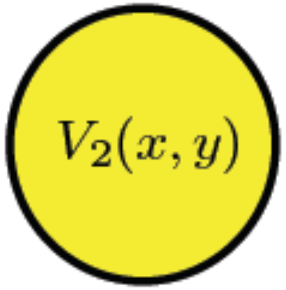

$$\nabla^2 V(x,y,z) = 0$$

$$\boxed{V(z=0) = V_1(x,y)}$$

$$F_{sp}(d) = 2\pi R \langle U_{pp}(d) \rangle = \frac{\epsilon_0 R}{16} \int_0^\infty dk \, \frac{k^2 e^{-kd}}{\sinh(kd)} \, [C_{1,k} + C_{2,k}]$$

Different models to describe surface potential fluctuations:

- $C_{1,k} = C_{2,k} = V_0^2 \text{ for } k_{\min} < k < k_{\max}$

$$F_{sp} = \frac{4\pi\epsilon_0 V_{\rm rms}^2 R}{k_{\max}^2 - k_{\min}^2} \int_{k_{\min}}^{k_{\max}} dk \frac{k^2 e^{-kd}}{\sinh(kd)}$$

(Speake and Trenkel, PRL 03).

- $\mathcal{R}(r) = \begin{cases} V_0^2 & \text{for } r \leq \lambda, \\ 0 & \text{for } r > \lambda. \end{cases}$

$$F_{sp} = 2\pi\epsilon_0 R \int_0^\infty du \; u \frac{J_1(u)}{e^{2ud/\lambda} - 1}$$

In the limit of large patches $(kd \ll 1)$:

$$\boxed{F_{sp}(d) = \pi\epsilon_0 R \, \frac{V_{\rm rms}^2}{d}}$$

Total Elec. Residual Force

We fit the data for the *residual force at the minimizing potential* with a force of electric origin, for distances $d > 5\mu\mathrm{m}$ (negligible Casimir)

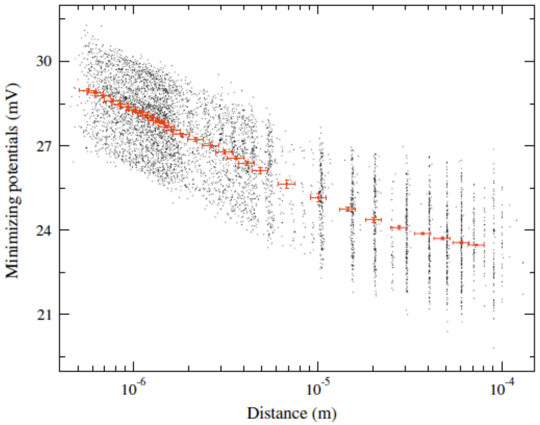

$$F_r^{\mathrm{el}}(d) = F_0 + \pi\epsilon_0 R \, \frac{[V_m(d) + V_1]^2 + V_{\mathrm{rms}}^2}{d}$$

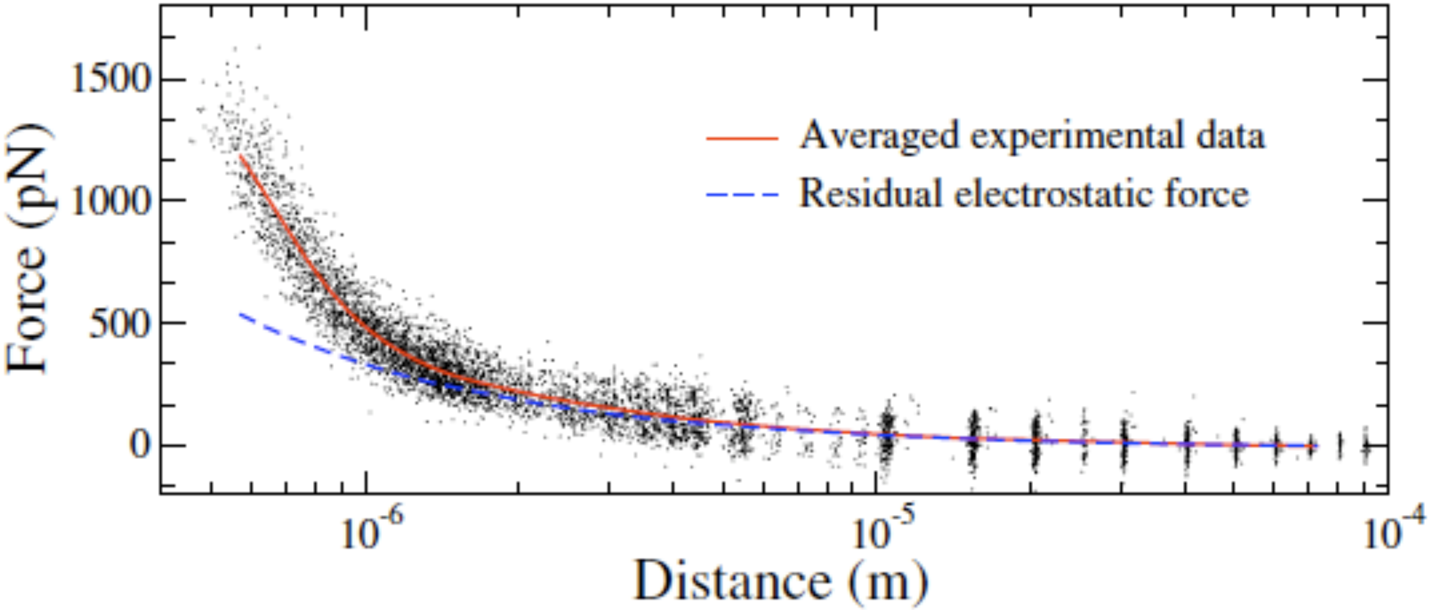

$$F_0 = (-11 \pm 2) \times 10^{-12}\ \mathrm{N}$$

$$V_1 = (-34 \pm 3)\ \mathrm{mV}$$

$$V_{\mathrm{rms}} = (6 \pm 2)\ \mathrm{mV}$$

$$\chi_0^2 = 1.5$$

Total Elec. Residual Force

Los Alamos NATIONAL LABORATORY

We fit the data for the *residual force at the minimizing potential* with a force of electric origin, for distances $d > 5\mu\mathrm{m}$ (negligible Casimir)

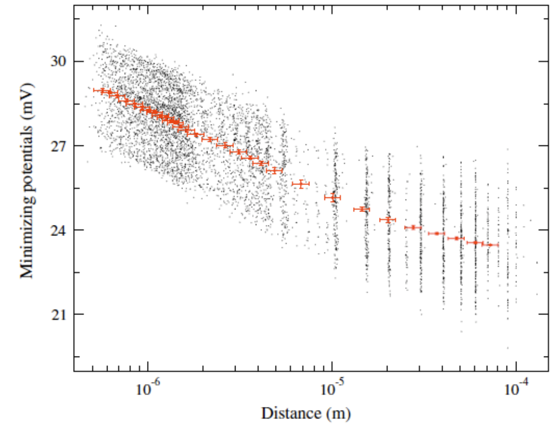

$$F_r^{\mathrm{el}}(d) = F_0 + \pi\epsilon_0 R \,\frac{[V_m(d) + V_1]^2 + V_{\mathrm{rms}}^2}{d}$$

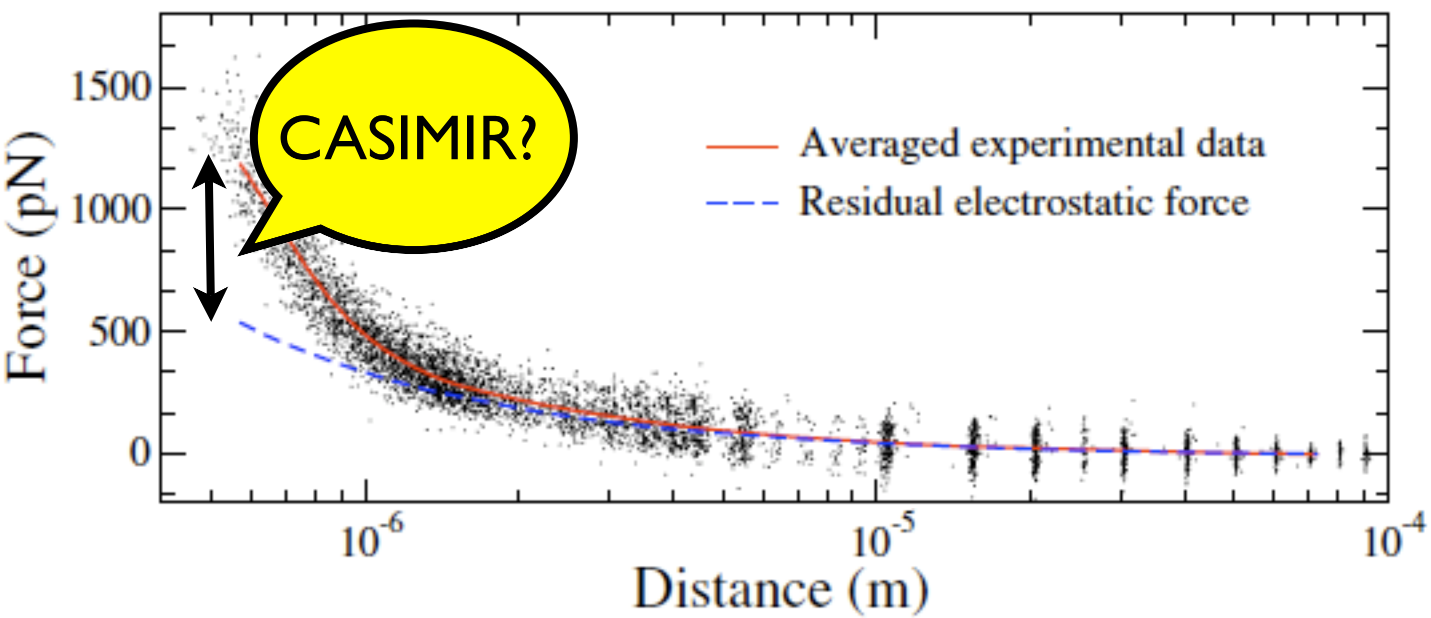

$$F_0 = (-11 \pm 2) \times 10^{-12}\ \mathrm{N}$$

$$V_1 = (-34 \pm 3)\ \mathrm{mV}$$

$$V_{\mathrm{rms}} = (6 \pm 2)\ \mathrm{mV}$$

$$\chi_0^2 = 1.5$$

Casimir with Ge: Theory

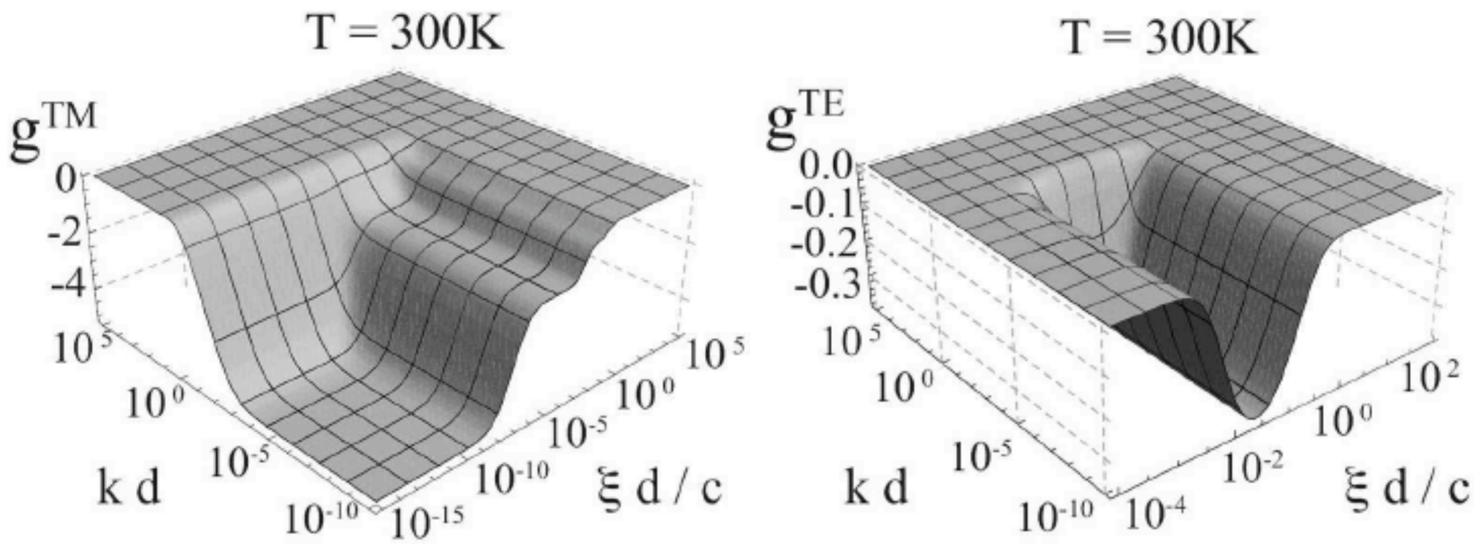

DD and Lamoreaux, PRL **101**, 163203 (2008)

DD and Lamoreaux, J. Phys. **161**, 012009 (2009)

Basic theory tools

- Casimir-Lifshitz pressure between two parallel plates:

$$P(d) = 2k_{\rm B}T \sum_{n=0}^{\infty}{}' \int \frac{d^2\mathbf{k}}{(2\pi)^2} \sqrt{k^2+\xi_n^2/c^2} \sum_{p={\rm TE,TM}} \frac{r_1 r_2 e^{-2d\sqrt{k^2+\xi_n^2/c^2}}}{1 - r_1 r_2 e^{-2d\sqrt{k^2+\xi_n^2/c^2}}}$$

$r_j = r^p_{\mathbf{k},j}(i\xi_n)$ reflection amplitudes

$\xi_n = 2\pi n k_{\rm B}T/\hbar$ Matsubara frequencies

- Casimir-Lifshitz free energy in the plane-plane geometry:

$$\frac{E}{A} = k_{\rm B}T \sum_p \sum_{n=0}^{\infty}{}' \int \frac{d^2\mathbf{k}}{(2\pi)^2} \ln[1 - r_1 r_2 e^{-2d\sqrt{k^2+\xi_n^2/c^2}}]$$

- Sphere-plane Casimir force is computed via PFA (well satisfied in the experiment)

$$F_{sp}(d) = 2\pi R U_{pp}(d) = 2\pi R \, \frac{E}{A}$$

Material properties of Ge

- intrinsic semiconductor, among the purest materials available
- small density of free carriers (electrons and holes)
- conductivity, thermal, and optical properties are well tabulated

Bare permittivity of intrinsic Ge
(not including contributions from free carriers)

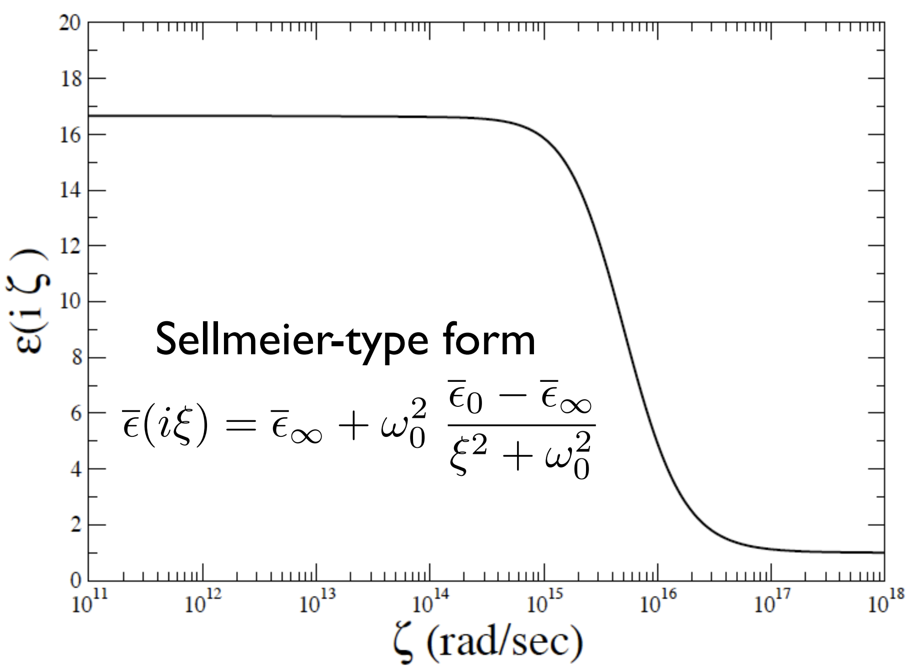

Conductivity properties of intrinsic Ge

Intrinsic carrier density: $n_0(T) = \sqrt{n_c n_v}\, e^{-\frac{E_g}{2k_B T}}$

$n_c(T)$ effect. density of states in conduction band

$n_v(T)$ effect. density of states in valence band

$E_g(T)$ energy band gap

At T=300K:

$$n_c = 1.04 \times 10^{-19}\ \mathrm{cm}^{-3}$$
$$n_v = 6.0 \times 10^{-18}\ \mathrm{cm}^{-3}$$
$$E_g = 0.66\ \mathrm{eV}$$

Carrier relaxation time: $\tau \approx 3.9\ \mathrm{ps}$

Effective mass of conduction electrons: $m_e = 0.12m$

Effective mass of conduction holes: $m_h = 0.21m$

Reflection Amplitudes. I

We need to compute the reflection amplitudes $r^{p}_{\mathbf{k},j}(\omega)$ for a vacuum-Ge interphase. Depending on the model used to describe the optical and conductivity properties of Ge we get different reflection amplitudes.

* Ideal dielectric model: No contribution from free carriers. Only the bare permittivity is taken into account. Reflection amplitudes are the usual Fresnel coefficients.

$$r^{\mathrm{TM}}_{\mathbf{k}}(i\xi) = \frac{\sqrt{k^2+\overline{\epsilon}(i\xi)\xi^2/c^2} - \overline{\epsilon}(i\xi)\sqrt{k^2+\xi^2/c^2}}{\sqrt{k^2+\overline{\epsilon}(i\xi)\xi^2/c^2} + \overline{\epsilon}(i\xi)\sqrt{k^2+\xi^2/c^2}} \qquad r^{\mathrm{TE}}_{\mathbf{k}}(i\xi) = \frac{\sqrt{k^2+\overline{\epsilon}(i\xi)\xi^2/c^2} - \sqrt{k^2+\xi^2/c^2}}{\sqrt{k^2+\overline{\epsilon}(i\xi)\xi^2/c^2} + \sqrt{k^2+\xi^2/c^2}}$$

* Ideal dielectric + Drude conductivity model: An ac Drude conductivity term is added to the bare permittivity.

$$\epsilon(i\xi) = \overline{\epsilon}(i\xi) + \frac{4\pi\sigma(i\xi)}{\xi}$$

$$\sigma(i\xi) = \sigma_0/(1+\xi\tau)$$

$$\sigma_0 = e^2 n_0 \tau/m_e \approx 1/(43\ \Omega\ \mathrm{cm})$$

Same Fresnel coefficients with the substitution $\overline{\epsilon}(i\xi) \longrightarrow \epsilon(i\xi)$

$$r^{\mathrm{TM}}_{\mathbf{k}}(\xi=0) = 1$$

$$r^{\mathrm{TE}}_{\mathbf{k}}(\xi=0) = 0$$

Reflection Amplitudes. II

✱ Quasi-static screening model: (Pitaevskii, PRL 08)

Takes into account the penetration of the static component of the fluctuating EM field into the material. Based on Debye-Huckel charge screening. Valid for small density of carriers. The relevant (longitudinal) Green function is expressed in terms of an auxiliary static potential field, that satisfies:

$$(\nabla^2 - \kappa^2)\varphi = 0 \qquad \kappa^2 = 4\pi e^2 n_0/\bar{\epsilon}_0 k_{\mathrm{B}} T$$

Debye radius: $R_D = 1/\kappa \approx 0.68\mu\mathrm{m}$ (for metals is much smaller, on the order of interatomic distances)

$$r_{\mathbf{k}}^{\mathrm{TE}}(\xi = 0) = 0 \qquad r_{\mathbf{k}}^{\mathrm{TM}}(\xi = 0) = \frac{\bar{\epsilon}_0 q - k}{\bar{\epsilon}_0 q + k} \qquad q = \sqrt{k^2 + \kappa^2}$$

(All other reflections coefficients for $\xi \neq 0$ are fixed to the case of the ideal dielectric model)

Effect of charge screening becomes important for distances $d > R_D$

✱ Charge-drift model: (DD and Lamoreaux, PRL 08)

Takes into account the interaction between drifting carriers in the semiconductor and traveling EM waves. Based on the classical Boltzmann transport equation, and valid for non-degenerate systems (small density of carriers) described by Maxwell-Boltzmann statistics.

Charge-drift model. I

Los Alamos NATIONAL LABORATORY

☑ Maxwell's eqns.:

$$\nabla \times \mathbf{E} = i\mu_0\omega\mathbf{H}, \quad \nabla \times \mathbf{H} = -i\overline{\epsilon}(\omega)\omega\mathbf{E} + \mathbf{J}, \quad \nabla \cdot \mathbf{E} = -\frac{en}{\overline{\epsilon}(\omega)}$$

$\mathbf{J} = -en\mathbf{v}$ carrier current

☑ Classical Boltzmann transport eqn.:

$$\left(\frac{\partial}{\partial t} + \mathbf{v} \cdot \nabla\right)\mathbf{v} = -\frac{e}{m}\mathbf{E} - \frac{v_T^2}{n}\nabla n - \frac{\mathbf{v}}{\tau}$$

$v_T = \sqrt{k_{\mathrm{B}}T/m}$ mean thermal velocity

Mixing both, we get the fundamental equation for the EM field inside the semiconductor:

$$\boxed{\left[\nabla^2 + \mu_0\overline{\epsilon}(\omega)\omega^2\left(1 + i\frac{\omega_c}{\omega(1-i\omega\tau)}\right)\right]\mathbf{E} = \left[1 + i\mu_0\overline{\epsilon}(\omega)\frac{\omega D}{1-i\omega\tau}\right]\nabla \cdot (\nabla \cdot \mathbf{E}).}$$

$\omega_c = 4\pi e n_0 \mu/\overline{\epsilon}(\omega)$

$\mu = e\tau/m$ mobility of carriers

$D = v_T^2\tau$ diffusion constant

Note: In the quasi-static limit, we recover Pitaevskii's screening results!

$$\omega_c/D = 4\pi e^2 n_0/\overline{\epsilon}(\omega)k_{\mathrm{B}}T \xrightarrow{\omega\to 0} 1/R_D^2$$

Charge-drift model. II

Solving the EM boundary conditions on the vacuum-Ge interphase, we obtain the following TE and TM reflection amplitudes

$$r_{\mathbf{k}}^{\mathrm{TM}}(i\xi) = \frac{\overline{\epsilon}(i\xi)\sqrt{k^2+\xi^2/c^2} - \chi}{\overline{\epsilon}(i\xi)\sqrt{k^2+\xi^2/c^2} + \chi},$$

$$r_{\mathbf{k}}^{\mathrm{TE}}(i\xi) = \frac{\sqrt{k^2+\xi^2/c^2} - \eta_T}{\sqrt{k^2+\xi^2/c^2} + \eta_T}.$$

$$\chi = \frac{1}{\eta_L}\left[k^2 + \overline{\epsilon}(i\xi)\frac{\xi^2}{c^2}\frac{\eta_L\eta_T - k^2}{\eta_T^2 - k^2}\right]$$

$$\eta_L(i\xi) = \sqrt{k^2 + \frac{4\pi e^2 n_0}{\overline{\epsilon}(i\xi) k_{\mathrm{B}} T} + \frac{\xi(1+\xi\tau)}{v_T^2 \tau}},$$

$$\eta_T(i\xi) = \sqrt{k^2 + [\overline{\epsilon}(i\xi) + 4\pi\sigma(i\xi)/\xi]\xi^2/c^2},$$

→ same as in the ideal dielectric+Drude conductivity model.

Some limiting behavior:

- In the quasi-static limit $\xi \to 0$ we recover Pitaevskii's results, namely

$r_{\mathbf{k}}^{\mathrm{TE}}(0) = 0$ (a static TE field is a purely magnetic field, fully penetrates a non-magnetic medium)

$r_{\mathbf{k}}^{\mathrm{TM}}(\xi = 0) = \dfrac{\overline{\epsilon}_0 q - k}{\overline{\epsilon}_0 q + k}$ (interpolates between a good conductor and an ideal dielectric)

- For $\xi \neq 0$ in the ideal dielectric limit (small free charge density and small thermal velocity), we recover Fresnel coefficients in terms of the bare permittivity $\overline{\epsilon}(\omega)$

Comparison of models

Given typical parameters for intrinsic semiconductors, $\omega_c/(1+\xi\tau)$ and $D\xi^{-1}/(1+\xi\tau)$ are very small in the relevant range of frequencies in the Lifshitz formula, and then only the $n=0$ TM mode is modified significantly. Thus, to very high accuracy, the effect of drifting carriers can be fully modelled by the Debye-Huckel screening length.

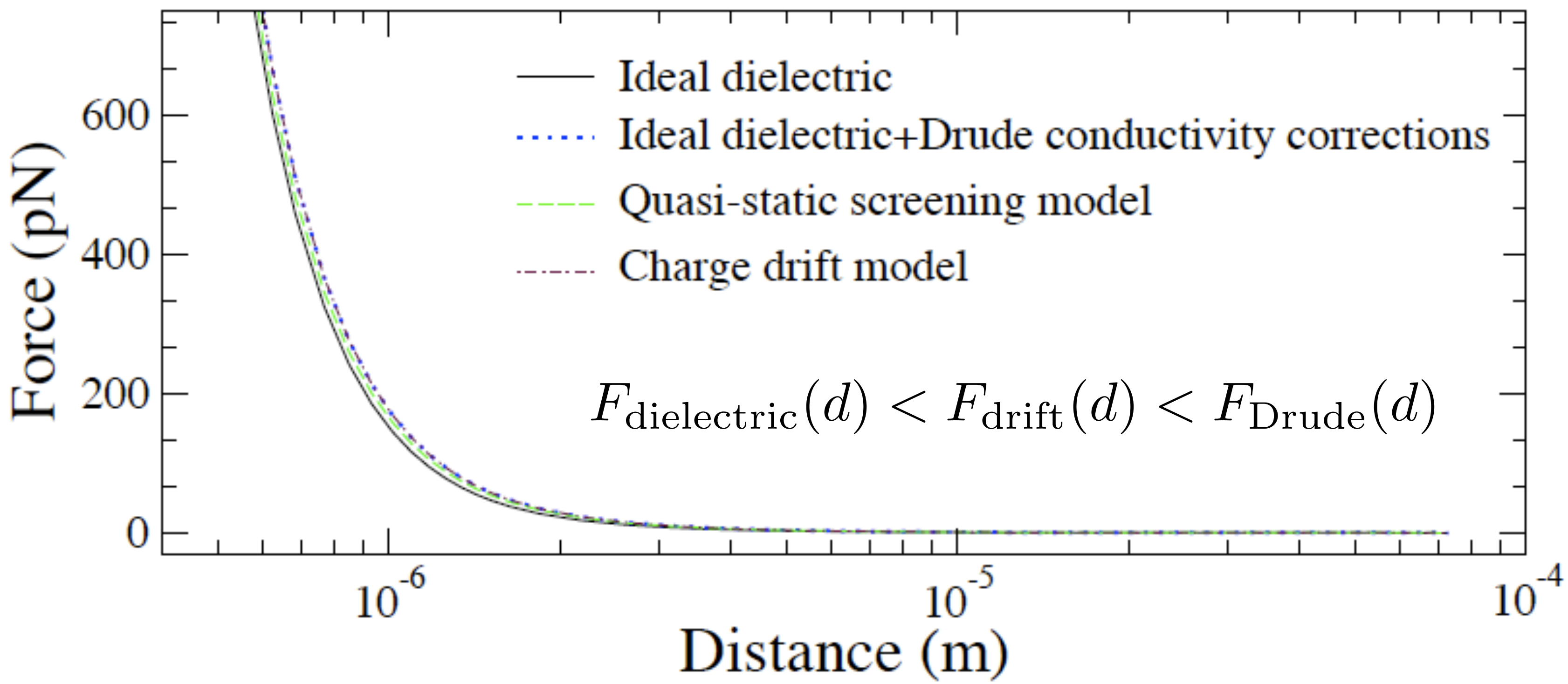

(See also Klimchitskaya, arXiv:0902.4254)

Digression I: Nernst theorem

Free energy: $E = \frac{\hbar}{2\pi} \sum_{p,\mathbf{k}} \sum_{n=0}^{\infty\prime} \theta g^p(in\theta, \mathbf{k}; \theta)$ $\qquad \theta = 2\pi k_{\mathrm{B}} T/\hbar$

Entropy: $S(\theta) = -\frac{2\pi}{\hbar} \frac{\partial E}{\partial \theta}$

$$g^p(\omega, \mathbf{k}; \theta) = \ln[1 - r^p_{\mathbf{k},1}(\omega, \theta)\, r^p_{\mathbf{k},2}(\omega, \theta) e^{-2d\sqrt{k^2-\omega^2/c^2}}]$$

Nernst theorem: $\boxed{S(T=0) = k_{\mathrm{B}} \ln \Omega_N}$

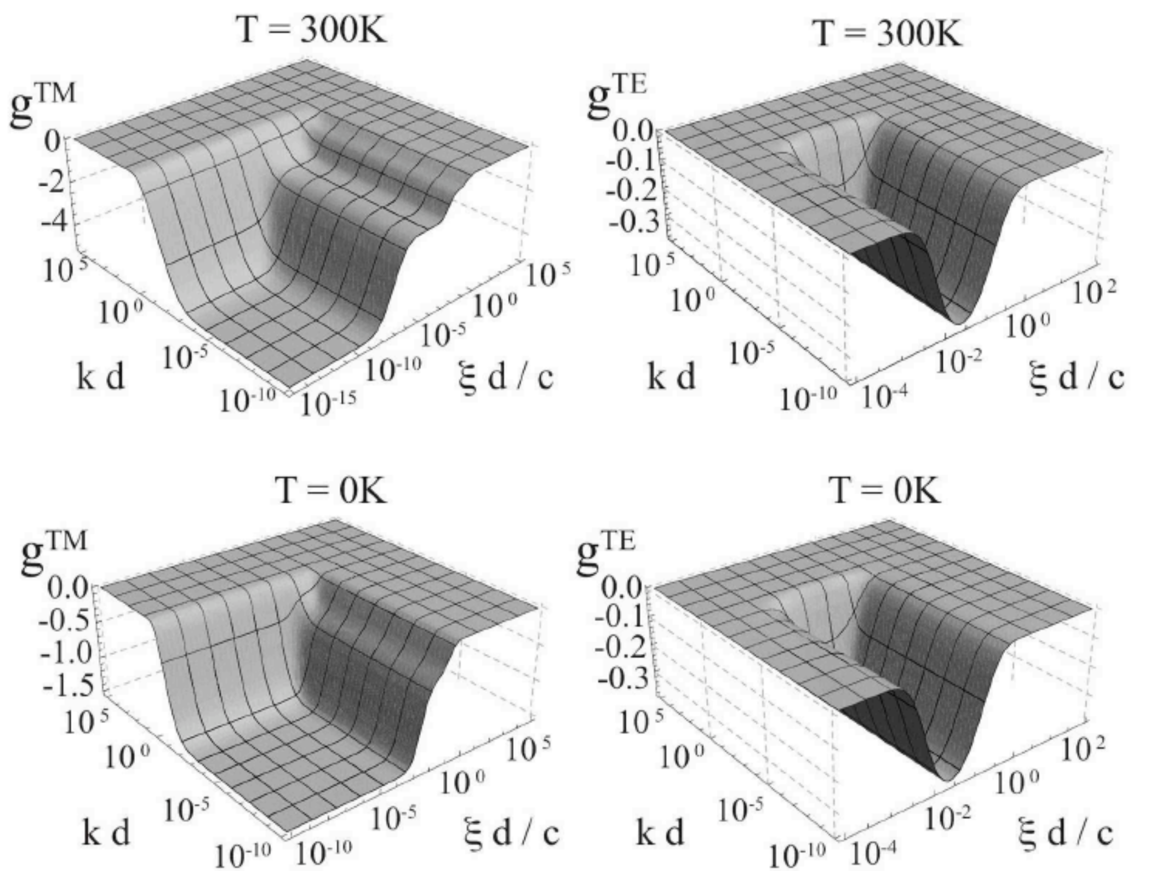

(Intravaia and Henkel, JPA 08)

We have shown that the charge drift model for intrinsic semiconductors verifies Nernst theorem with $\Omega_N = 1$

$$n_0(T) \propto e^{-1/T} \text{ for } T \to 0$$

(DD and Lamoreaux, J. Phys. 09)

Digression II: Spatial Dispersion

Los Alamos NATIONAL LABORATORY

- Pitaevskii's quasi-static screening model can be cast in the form of spatial dispersion

static permittivity tensor $\epsilon = \mathrm{diag}(\epsilon^{\perp}, \epsilon^{\perp}, \epsilon^{\|})$

$$\epsilon^{\perp} = \overline{\epsilon}_0$$

$$\epsilon^{\|}(k) = \overline{\epsilon}_0[1 + 1/(kR_{\mathrm{D}})^2]$$

Computing the reflection coefficients for an anisotropic (uniaxial) material one recovers the static reflection amplitudes:

$$r_{\mathbf{k}}^{\mathrm{TE}}(\xi = 0) = 0 \qquad r_{\mathbf{k}}^{\mathrm{TM}}(\xi = 0) = \frac{\overline{\epsilon}_0 q - k}{\overline{\epsilon}_0 q + k}$$

- Similarly, our charge drift model can also be cast in terms of spatial dispersion

Express reflection amplitudes $r_{\mathbf{k}}^{p}(\omega)$ in terms of permittivity tensor $\epsilon(\omega, k)$

(Sernelius, PRB 05; Esquivel-Sirvent et al, JPA 06)

$$\epsilon^{\|}(k, i\xi) = \frac{k}{\gamma^0} \times \left[\frac{\overline{\epsilon}(i\xi)\gamma^0}{\chi} - 1 + \frac{k}{\gamma^0} + \frac{\xi^2/c^2}{\gamma^0}\left(\frac{1}{\eta_T} - \frac{1}{\gamma^0}\right) + \frac{k\xi^2/c^2}{\gamma^0}\left(\frac{1}{k\eta_T - \eta_T^2} - \frac{1}{k\gamma^0 - (\gamma^0)^2}\right)\right]^{-1}$$

$$\gamma^0 = \sqrt{k^2 + \xi^2/c^2}$$

$$\eta_T = \sqrt{k^2 + \epsilon^{\perp}(k, i\xi)\xi^2/c^2}$$

$$\epsilon^{\perp}(k, i\xi) = \overline{\epsilon}(i\xi)\left[1 + \frac{\omega_c}{\xi(1 + \xi\tau)}\right]$$

(DD and Lamoreaux, J. Phys. 09)

Casimir with Ge: Experiment

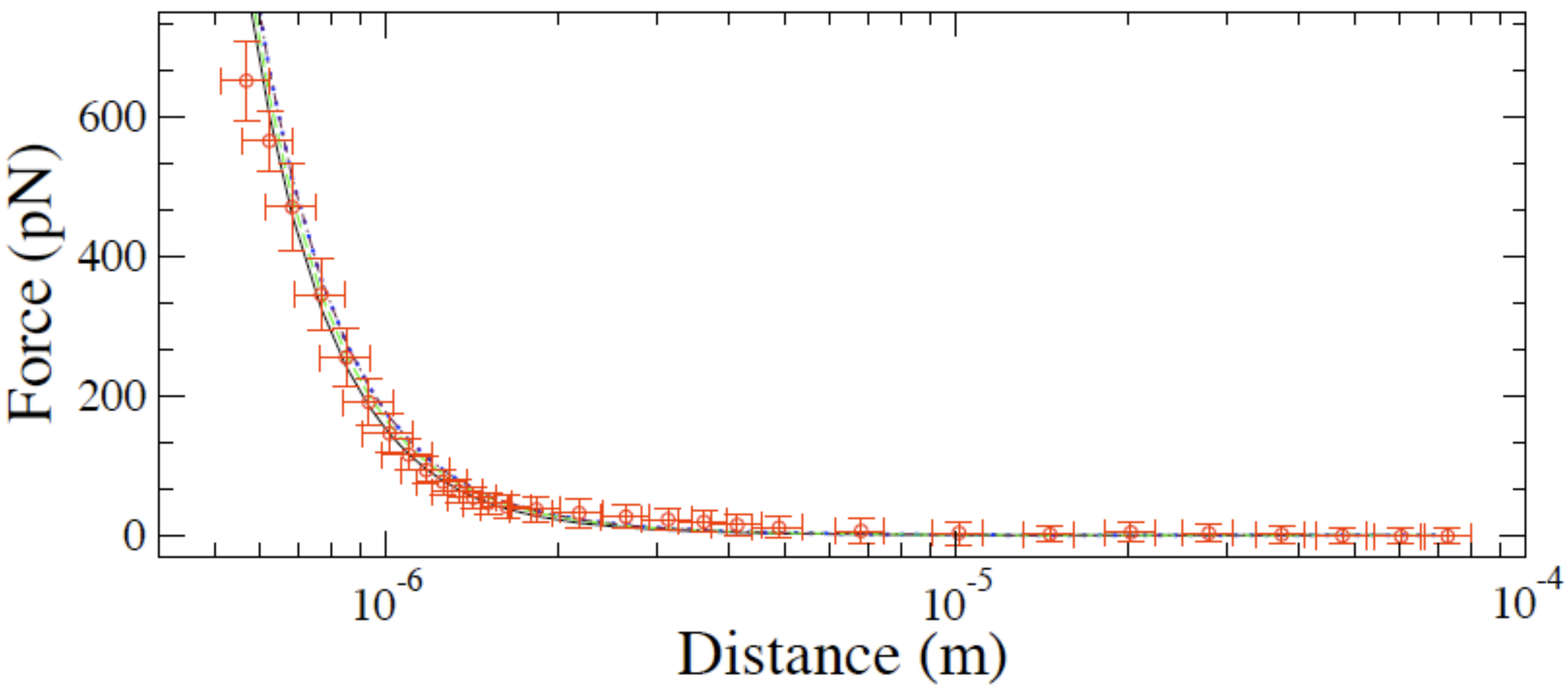

Kim, Sushkov, DD, Lamoreaux, PRL **103**, 060401 (2009)

Casimir force residuals

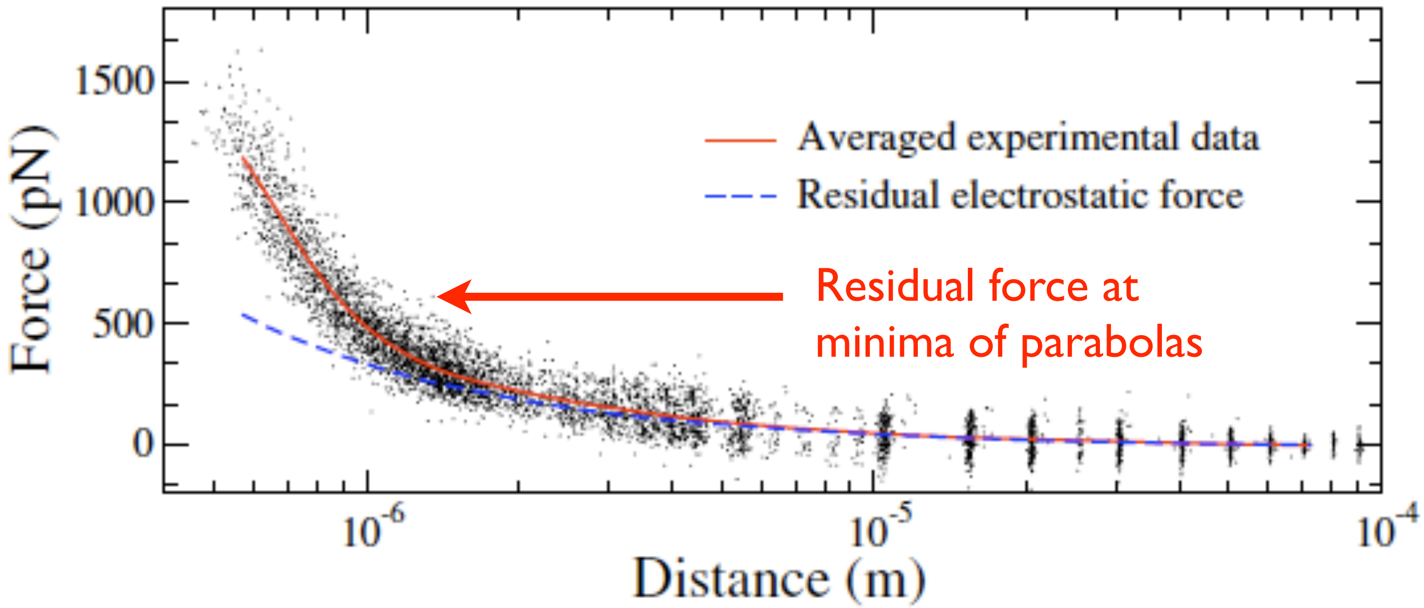

Casimir force residuals

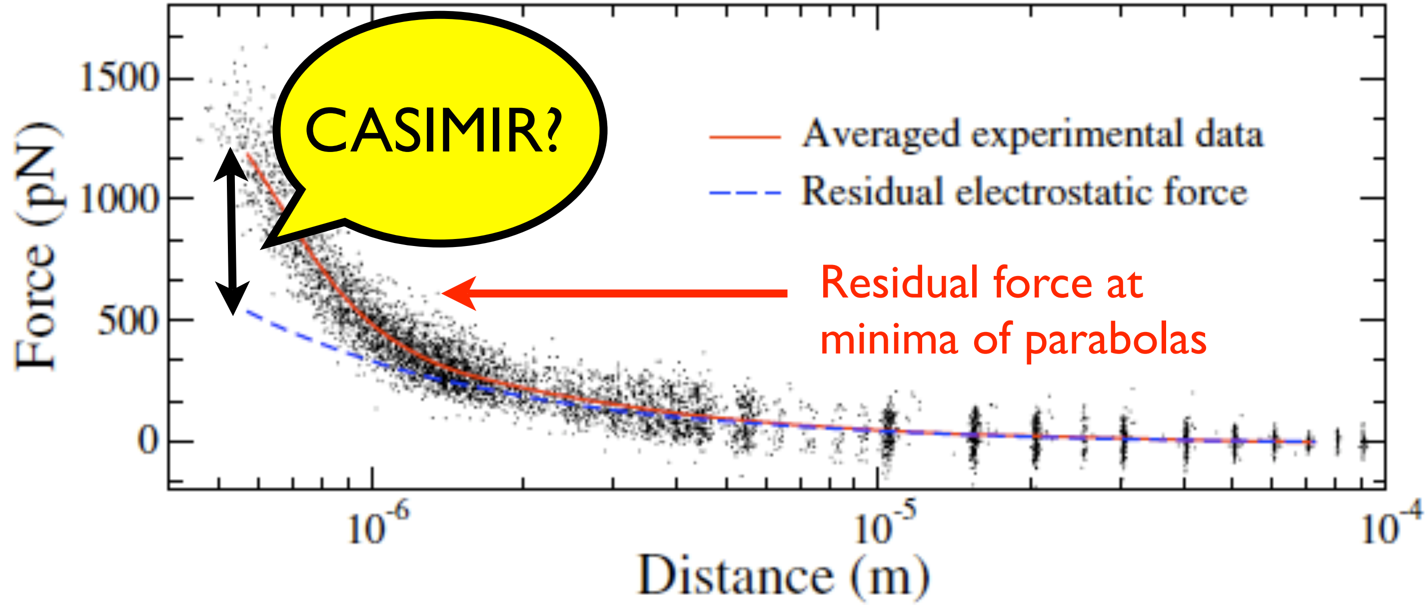

Casimir force residuals

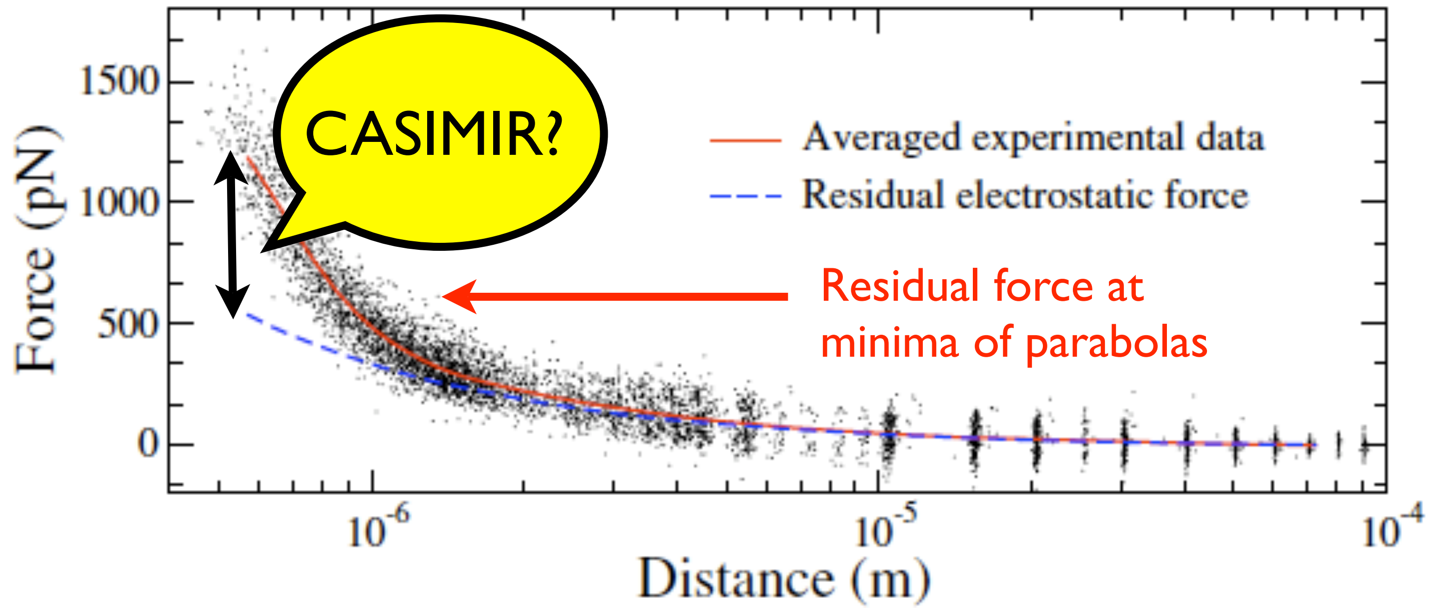

After subtraction of the electrostatic force residual $F_r^{\mathrm{el}}(d) = F_0 + \pi\epsilon_0 R\,\frac{[V_m(d)+V_1]^2 + V_{\mathrm{rms}}^2}{d}$

Casimir force residuals

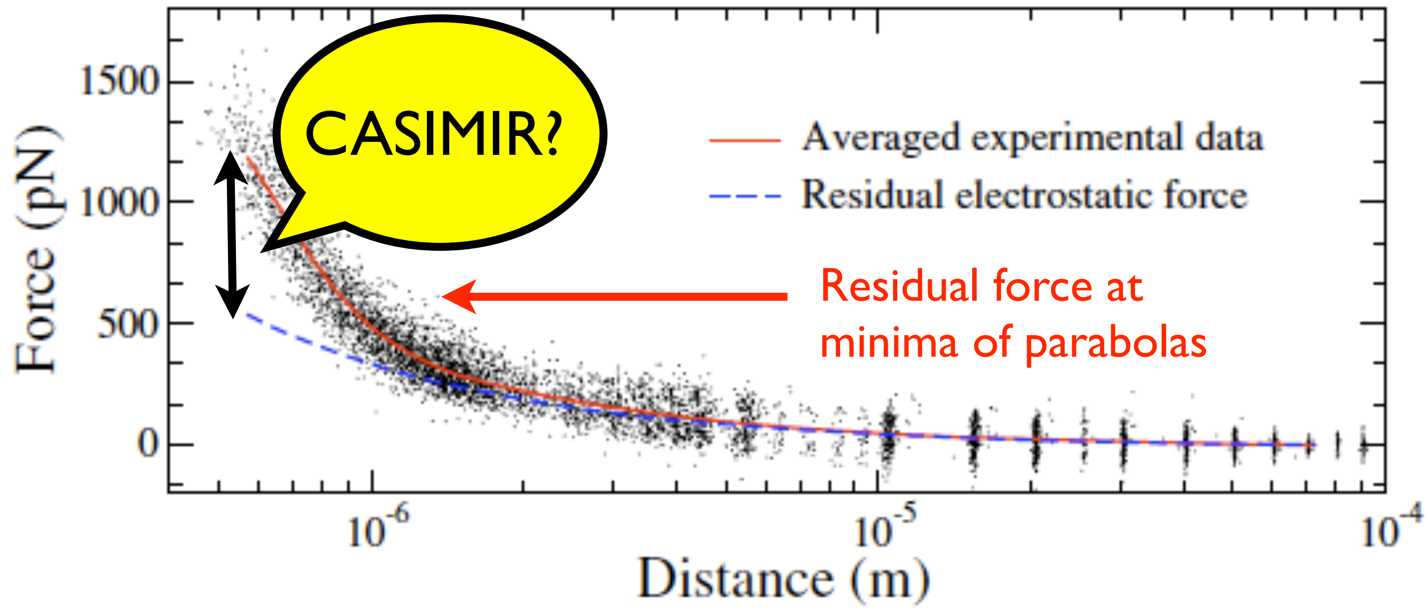

After subtraction of the electrostatic force residual $F_r^{\mathrm{el}}(d) = F_0 + \pi\epsilon_0 R\,\frac{[V_m(d)+V_1]^2 + V_{\mathrm{rms}}^2}{d}$

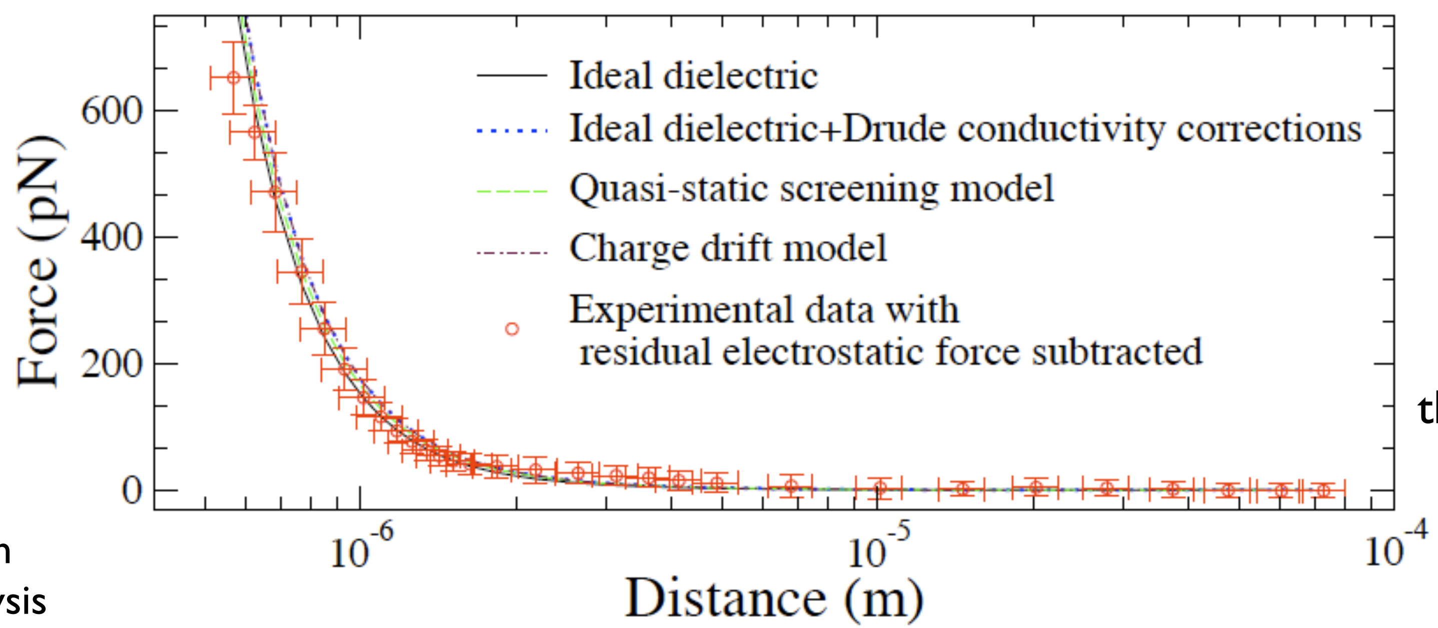

Error bars:

3% statistical uncertainties

10% fitting uncertainties from electrostatic analysis

For $d < 5\mu\mathrm{m}$

$\chi_0^2 \approx 1$

for all the theoretical models

Remarks on the Ge experiment

- Found a distance-dependent minimizing potential, due to large-scale variations in the contact potential along the surface of the plates. It results in a relatively large residual force of electrostatic origin $\propto [V_m(d) + V_1]^2/d$

- Found another residual force of electrostatic origin, probably due to potential patches on the surfaces that, for $d \ll \lambda \ll R$, is $\propto V_{\rm rms}^2/d$

- After subtraction of these two electrostatic residuals, we got very good agreement with a Casimir force residual. However, we do not have enough accuracy to distinguish between the different theoretical models.

- Further measurements deemed necessary to better understand the origins of the observed residual electrostatic force. For example, Kelvin probe measurements of the potential patches on the samples.

Casimir with Au: new experiment

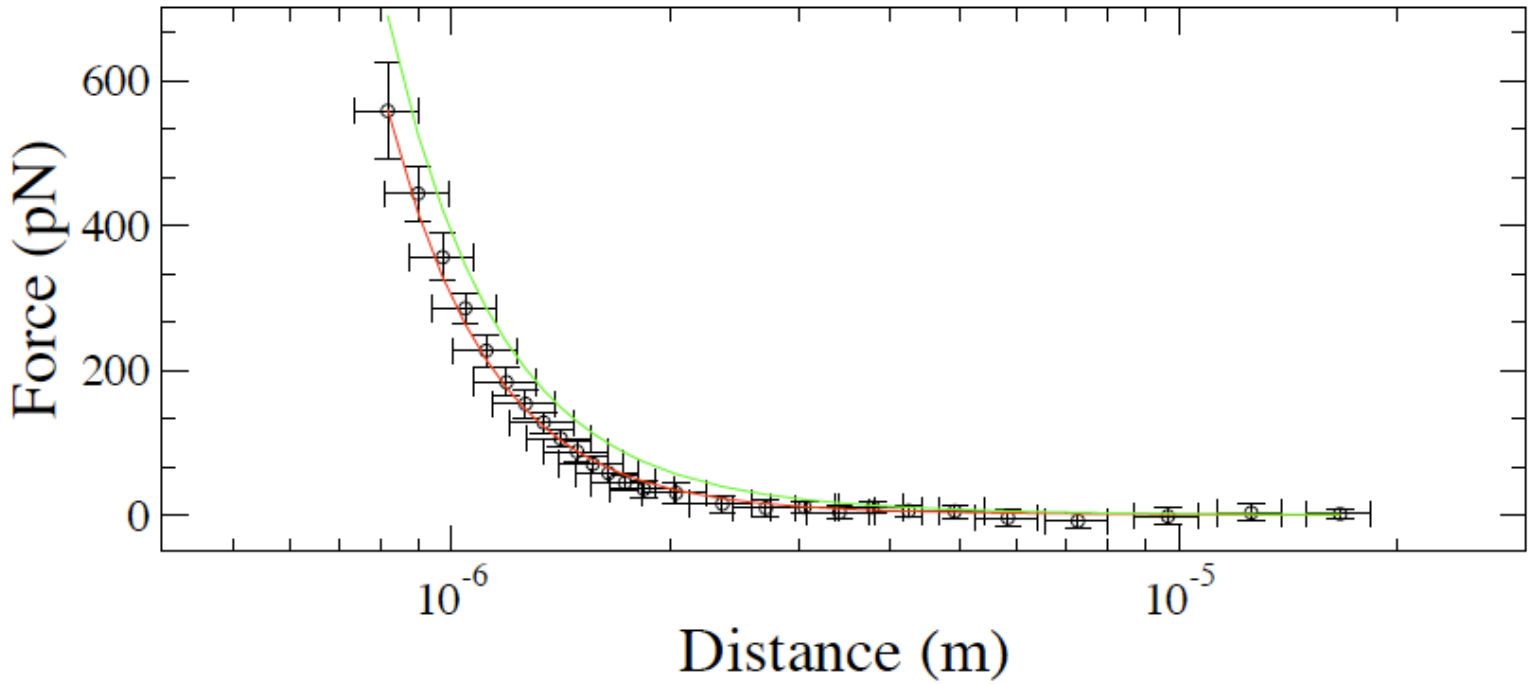

Kim, Sushkov, DD, Lamoreaux, work in progress

Ongoing Au experiment (Prelim)

Los Alamos NATIONAL LABORATORY

We are performing a new experiment with Au samples in the sphere-plane configuration using the same torsional pendulum set-up

$R = 15.45\ \mathrm{cm}$ (slightly larger than the sphere for the Ge measurements)

Same calibration procedure as in the Ge experiment is followed:

- Curvature parameter $k(d)$: From the curvature of the electrostatic parabolas we obtain the force-voltage calibration constant and the absolute distance

$\beta = (1.27 \pm 0.04) \times 10^{-7}\ \mathrm{N/V}$ (slight difference with the Ge case attributable to different Au and Ge masses)

$$k(d) = \frac{\pi \epsilon_0 R/\beta}{d}$$

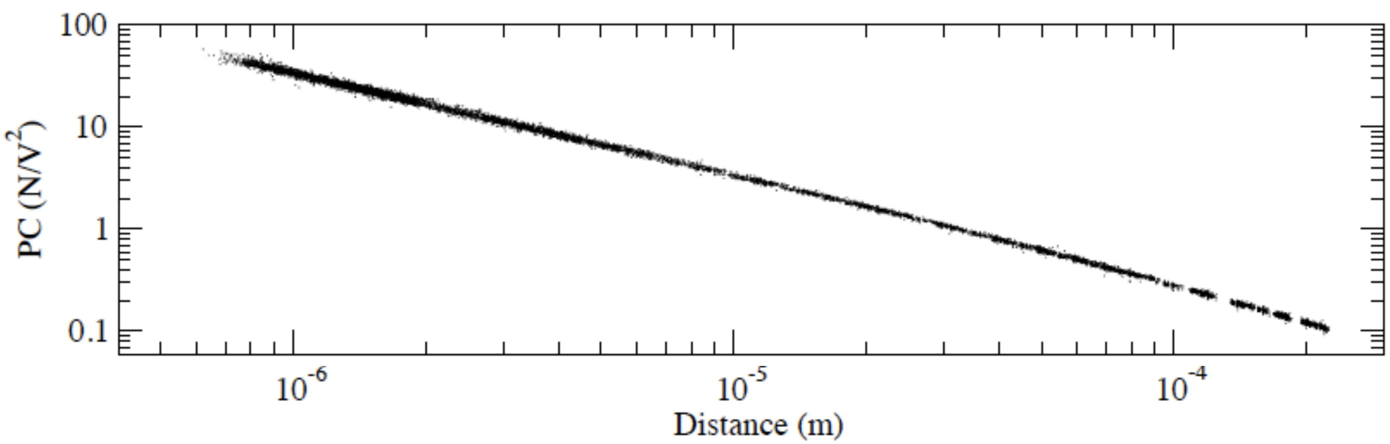

Ongoing Au experiment (Prelim)

- Varying minimizing potential $V_m(d)$: Quite different behavior from the Ge case.

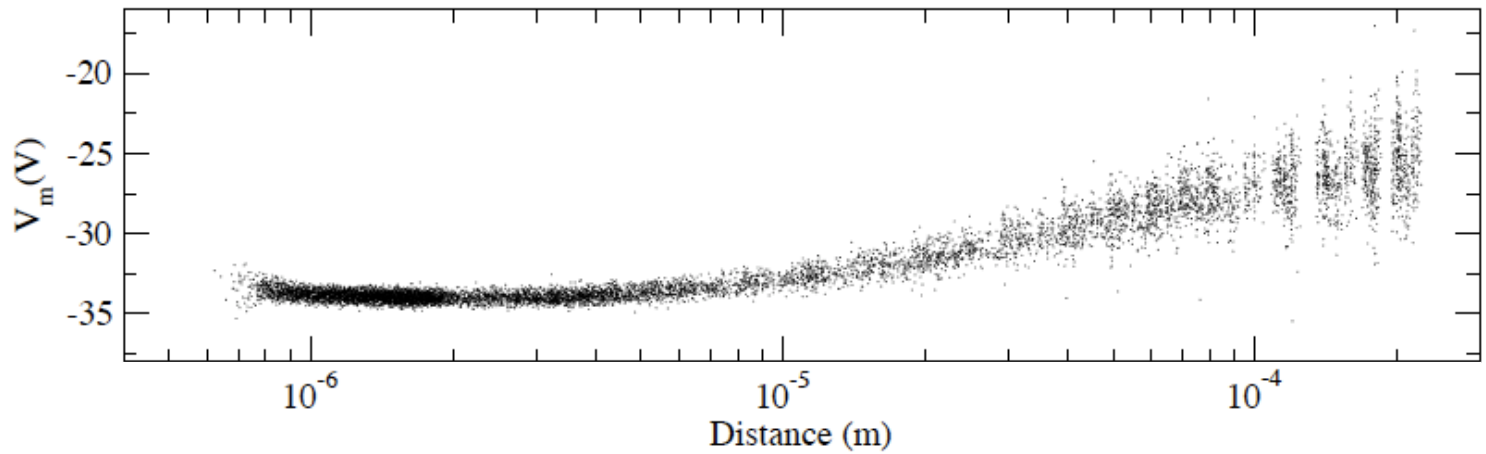

- Force residuals: value of measured signal at the minima of each parabola

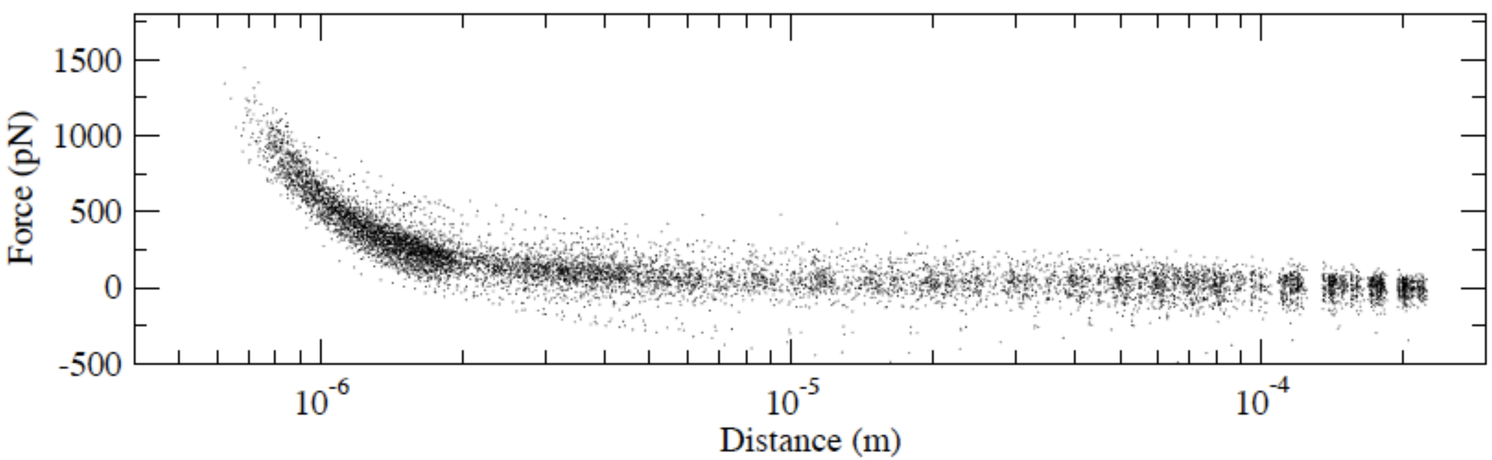

Ongoing Au experiment (Prelim)

We perform a fit of the force residuals to look for possible electrostatic potential patch effects

$$F_r^{\mathrm{el}}(d) = F_0 + \pi\epsilon_0 R \, \frac{[V_m(d) + V_1]^2 + V_{\mathrm{rms}}^2}{d}$$

$$\begin{aligned} V_m(d) &\approx -34 \text{ mV} \\ V_1 &\approx -V_m(d) \\ V_{\mathrm{rms}} &\approx (7 \pm 1) \text{ mV} \\ F_0 &= (2.5 \pm 0.4) \times 10^{-11} \text{ N} \end{aligned}$$

and then subtract it from the force residuals. We then get new force residuals (circles) that we compare against Casimir theory.

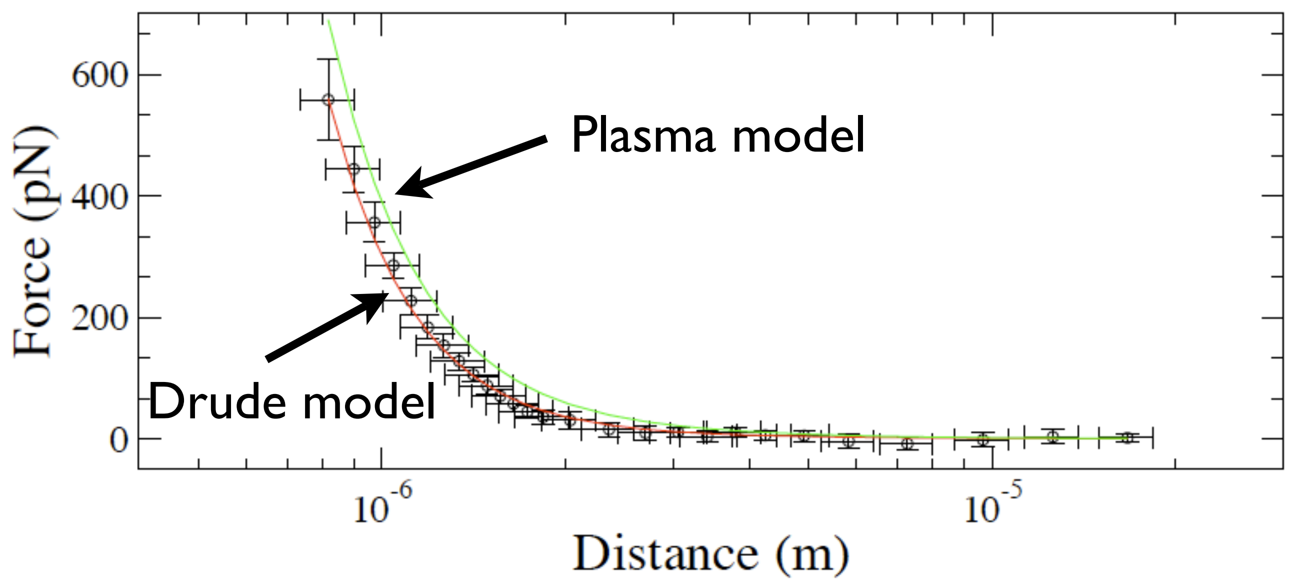

Ongoing Au experiment (Prelim)

Los Alamos NATIONAL LABORATORY

Theoretical modeling:

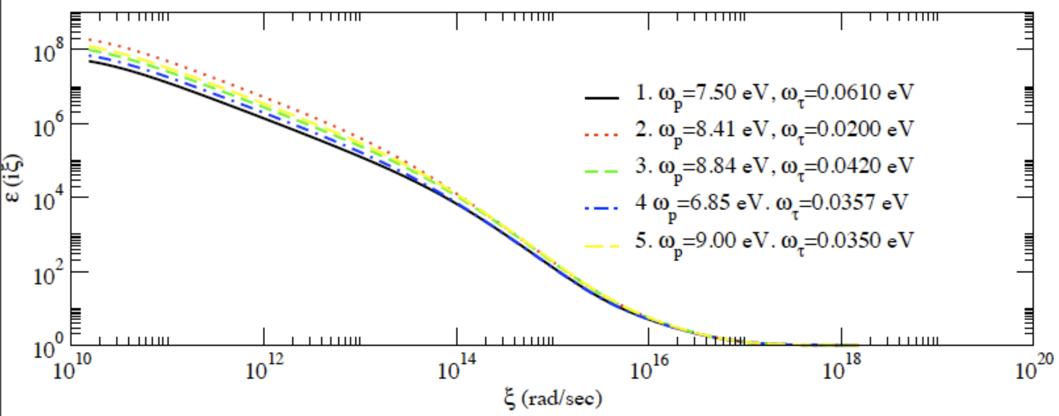

Sample dependence (beyond our accuracy)

Drude model: optical data extrapolated to zero frequency according to

$$\epsilon(\omega) = 1 - \frac{\omega_p^2}{\omega(\omega + i\omega_\tau)} \rightarrow \begin{array}{l} r_{\mathbf{k}}^{\mathrm{TM}}(\xi = 0) = 1 \\ r_{\mathbf{k}}^{\mathrm{TE}}(\xi = 0) = 0 \end{array}$$

Plasma model: optical data extrapolated to zero frequency according to

$$\epsilon(\omega) = 1 - \frac{\omega_p^2}{\omega^2} \rightarrow \begin{array}{l} r_{\mathbf{k}}^{\mathrm{TM}}(\xi = 0) = 1 \\ r_{\mathbf{k}}^{\mathrm{TE}}(\xi = 0) = \dfrac{k - \sqrt{k^2 + \omega_p^2/c^2}}{k + \sqrt{k^2 + \omega_p^2/c^2}} \end{array}$$

Ongoing Au experiment (Prelim)

Los Alamos NATIONAL LABORATORY

Theoretical modeling:

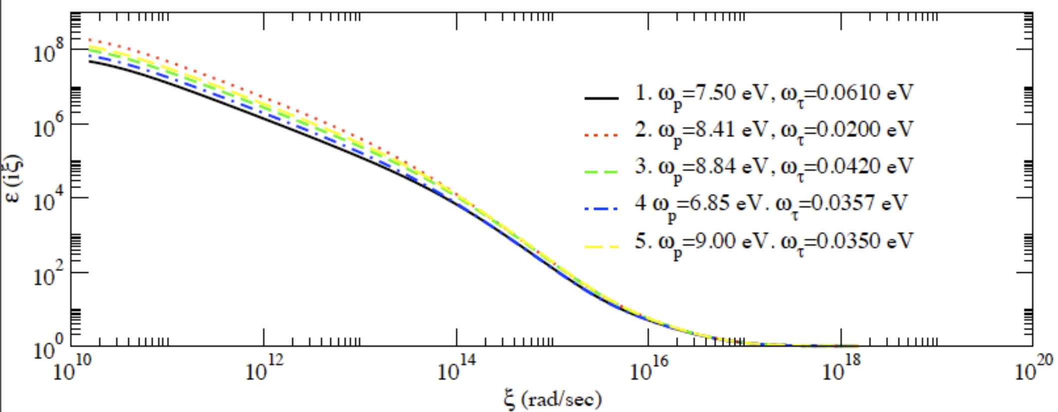

Sample dependence (beyond our accuracy)

Drude model: optical data extrapolated to zero frequency according to

$$\epsilon(\omega) = 1 - \frac{\omega_p^2}{\omega(\omega + i\omega_\tau)} \rightarrow \begin{array}{l} r_{\mathbf{k}}^{\mathrm{TM}}(\xi = 0) = 1 \\ r_{\mathbf{k}}^{\mathrm{TE}}(\xi = 0) = 0 \end{array}$$

Plasma model: optical data extrapolated to zero frequency according to

$$\epsilon(\omega) = 1 - \frac{\omega_p^2}{\omega^2} \rightarrow \begin{array}{l} r_{\mathbf{k}}^{\mathrm{TM}}(\xi = 0) = 1 \\ r_{\mathbf{k}}^{\mathrm{TE}}(\xi = 0) = \dfrac{k - \sqrt{k^2 + \omega_p^2/c^2}}{k + \sqrt{k^2 + \omega_p^2/c^2}} \end{array}$$

Preliminary analysis suggests that Drude model is correct (better χ_0^2 than the plasma model)

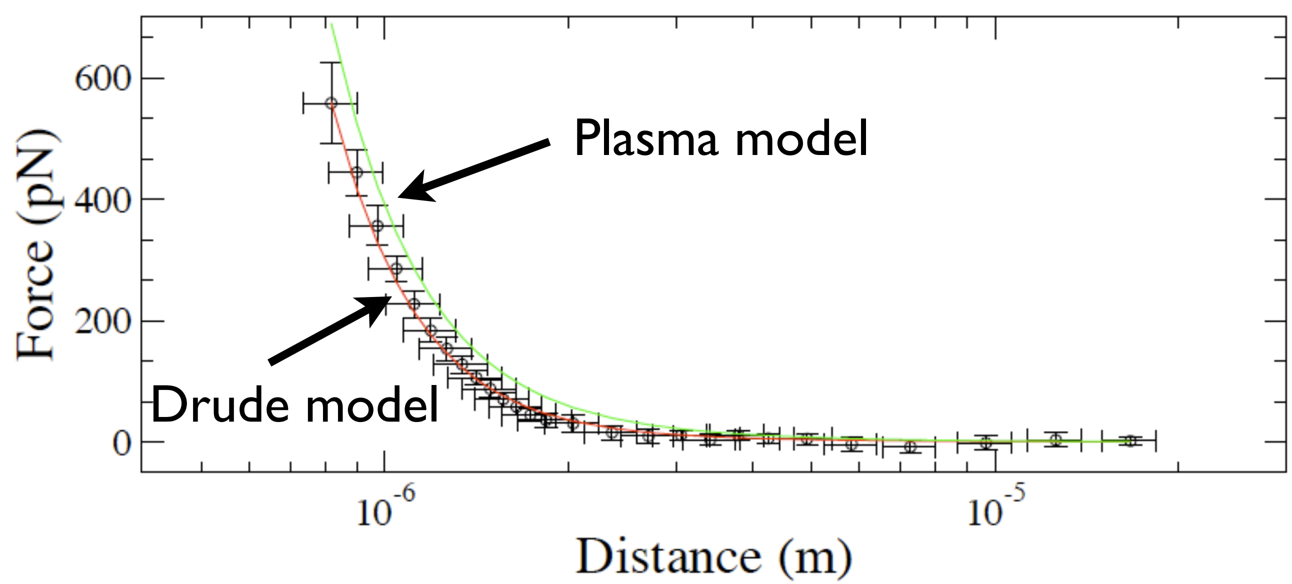

Remarks on the Au experiment

- Au measurements and preliminary analysis completed; suggests Drude model is correct. Further analysis with Kelvin probe microscopy would be extremely valuable.

- Lamoreaux's 1997 Au torsion pendulum experiment was most likely contaminated by the varying minimizing potential (such systematic was not taken into account then). This made the Casimir force larger than expected based on the Drude model.

- The Drude model predicts a Casimir force weaker than the Plasma model. Corrections from incorrect $1/d$ subtraction make the experimentally measured force larger than the Casimir force alone.

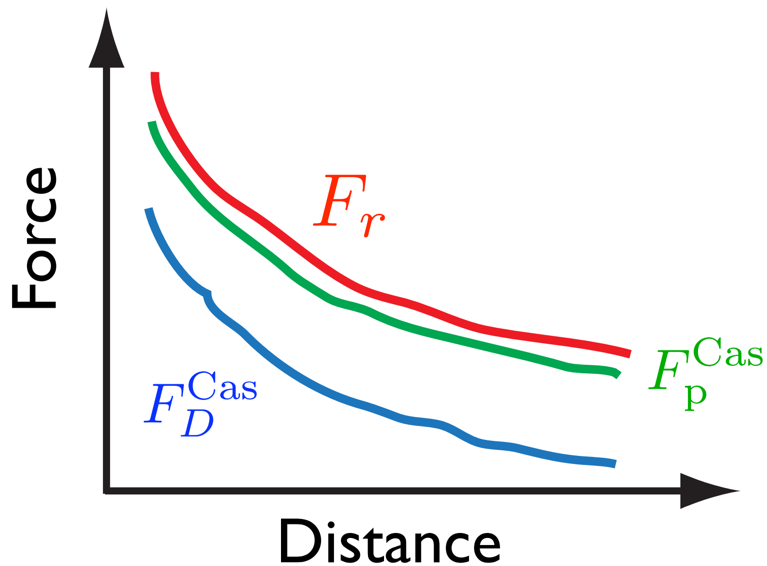

Remarks on the Au experiment

Los Alamos NATIONAL LABORATORY

- Au measurements and preliminary analysis completed; suggests Drude model is correct.

- Lamoreaux's 1997 Au torsion pendulum experiment was most likely contaminated by the varying minimizing potential (such systematic was not taken into account then). This made the Casimir force larger than expected based on the Drude model.

- The Drude model predicts a Casimir force weaker than the Plasma model. Corrections from incorrect $1/d$ subtraction make the experimentally measured force larger than the Casimir force alone.

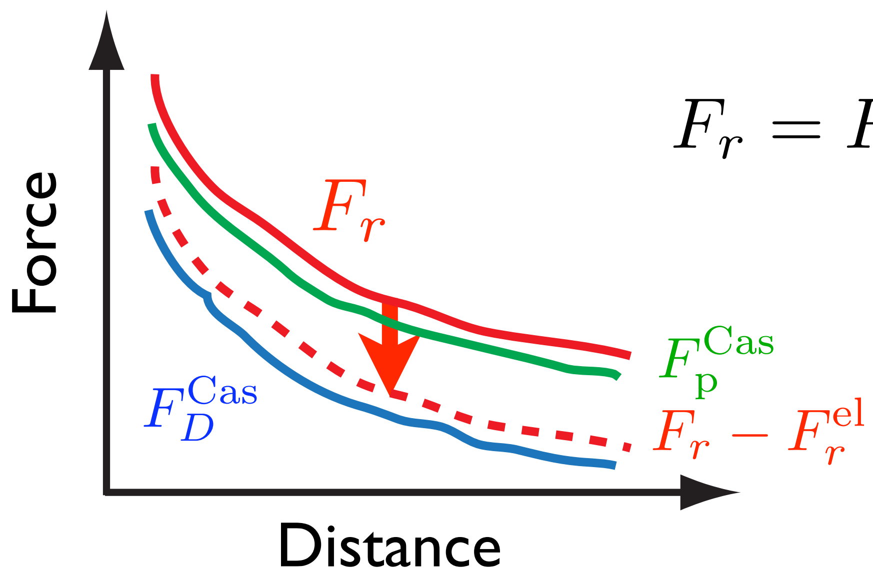

$$F_r = F_r^{\mathrm{el}} + F_r^{\mathrm{Cas}} + \ldots$$

References

- Theory of Casimir forces with Ge plates

  DD and Lamoreaux, PRL **101**, 163203 (2008)

  DD and Lamoreaux, J. Phys. **161**, 012009 (2009)

- Theory of potential patches, elec. calibrations, and Casimir force measurements

  Kim, Sushkov, DD, Lamoreaux, arXiv:0905.3421

- Experiment on Casimir forces with Ge plates

  Kim, Sushkov, DD, Lamoreaux, PRL **103**, 060401 (2009)

http://cnls.lanl.gov/casimir

See you in Santa Fe!